S 543

LINKAGE-CURRENT DIAGRAM FOR REPRESENTING MAGNETO OPERATION

By F. B. Silsbee and D. W. Randolph

ABSTRACT

This paper puts forward a diagram on which the electromagnetic cycle of operations, which leads to the production of a spark by a magneto or induction coil, can be represented in detail. Areas on the diagram correspond to the energy changes involved. It therefore is in a way analogous to the "pressure-volume" or the "temperature entropy" diagram so widely used in thermodynamic studies.

Methods are given for plotting the diagram from data of various kinds, and sample diagrams are shown. In the appendix is given a detailed mathematical discussion of the oscillations which can occur in the case when a circuit containing inductance, capacitance, and resistance is coupled to another containing inductance and resistance only. This combination is similar to the system existing when eddy currents in the core or when the currents flowing in the spark or in the carbon deposit on a fouled spark plug react on the current in the magneto winding.

CONTENTS

	Page
I. Introduction	648
II. The diagram	649
III. Methods for plotting	659
IV. Typical diagrams	667
V. Conclusions	674
VI. Notation	674
VII. Appendixes	676
A. Proof of energy relation	676
B. Definitions of ratio	677
C. Current relations in an oscillating circuit with a closed secondary	679
(*a*) General equations	680
(*b*) Application to effect of eddy currents	688
(*c*) Application to effect of shunting conductance on secondary	691
(*d*) Application to transfer of energy from primary to secondary	692
D. Eddy currents in induction coils	696

I. INTRODUCTION

The spark which jumps across the gap of a spark plug in an engine cylinder is the climax of a series of events which must happen inside the magneto in just the right way in order that the spark may occur. In studying the operation of a magneto it is very desirable to have a means for representing to the eye such a sequence of events and particularly the magnitude of the energy transformations which occur. It is the purpose of this paper to describe such a form of representing the phenomena which has been found useful in the work on spark generators now under way at the Bureau of Standards.

In studying the operation of either the steam engine or the internal-combustion engine it has been found very convenient to make use of certain diagrams, such as the pressure-volume diagram (or indicator "card") and the temperature-entropy diagram. Such diagrams owe their usefulness to the two important properties which they possess—(1) areas on the diagrams are proportional to energy changes, either in the form of work or heat; (2) a point on the diagram indicates by its location the state of the system (or of the working fluid) at any instant. In the case of a magneto or spark coil, a diagram in which the flux turns linking the winding is plotted as ordinate against the current flowing in the winding as abscissa has these same two properties, and it is hoped that it will prove as useful.

The cycle of operation which is passed through by the magneto for each spark has been described at some length in National Advisory Committee for Aeronautics Technical Report No. 58. It may be divided into six periods, each of which is separated from the preceding and following periods by an abrupt change in the circuit conditions. During period 1 the primary circuit is closed and the rotation of the armature establishes a considerable current in the primary winding. The breaker contacts then open, and during period 2 the stored magnetic energy is changed in part to electrostatic form and raises the secondary terminal to high potential. The spark gap then breaks down, and during period 3 this electrostatic energy is dissipated with great rapidity in the spark gap. The gap remains conducting for an appreciable time after the capacitance has been discharged, and during this period (4) additional magnetic energy is dissipated as heat in the spark gap. The breaker points then close and the spark (if it has not already died out) is extinguished by the reaction of the primary circuit on the secondary during period 5. The armature then continues to rotate with negligible current flow during period 6 until the position of maximum flux is reached and period 1 of the next cycle begins.

II. THE DIAGRAM

In the simplest case of an air-core inductance coil with a single winding, a graph of flux linkages plotted against current in the coil is merely a straight line, as shown by $O\ A$ in Figure 1. When the current is $O\ B$, the flux turns are $A\ B$, and point A indicates the state of the system at this instant. If the current is reduced to $O\ F$, the state point moves to D. The magnetic energy transformed

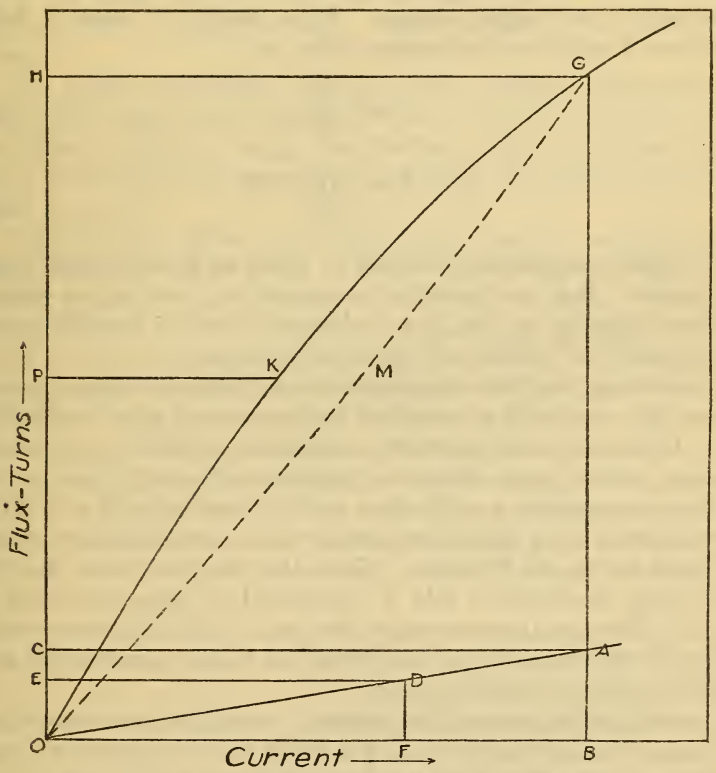

FIG. 1.—*Typical flux-turn current diagram for induction coil*
O A is graph for an air-core coil. *O G* is graph for an iron-core coil

into electrical work during such a change can be shown (see Appendix A) to be proportional to the area $C\ A\ D\ E$; that is, to the area between the vertical axis and the line representing the path of the state point between the initial and final positions. This relation holds true whether the transition from one state to the other be slow or rapid.

In the state represented by A the total energy available on breaking the circuit is the area of the triangle $C\ A\ O$. In this simple

case it is customary to define the self-inductance L as the slope of the line $O\ A$ and the total energy is seen to be

$$W = \tfrac{1}{2}\, LI^2 \tag{1}$$

However, if the magnetic circuit contains iron, the permeability of which varies with the flux density the $N\ \phi$–I graph becomes curved as at $O\ K\ G$. The total energy available for a current $O\ B$ is the approximately triangular area $H\ G\ K\ O$. In such a case the inductance is no longer constant. It is possible to make a fresh definition of equivalent inductance either as

$$L' = \frac{G\ B}{O\ B} \tag{2}$$

or as

$$L'' = \frac{2\ area\ H\ G\ K\ O}{OB^2} \tag{3}$$

These values, in general, will not be equal and will depend upon the current. It is for many purposes simpler, however, to express relations directly on the $N\ \phi$–I diagram than to introduce such "equivalent" or "effective" values of inductance.

Hysteresis in the iron core introduces a further complication and renders the value of $N\ \phi$ dependent on past as well as present values of I. However, in the operation of any form of ignition system the magnetic circuit passes through a succession of equal cycles so that the iron soon reaches a cyclic state and the relation of $N\ \phi$ to I can be represented by a single loop, as shown by combining the dotted and solid curves in Figure 1. Thus, the electrical work done in establishing the magnetic field is represented by the area $O\ M\ G\ H$, and the difference (represented by the loop $O\ M\ G\ K$) between this and the available energy is the amount of energy transformed into heat by hysteresis loss in the iron.

In most ignition systems the magnetic circuit contains an air gap of considerable reluctance with the result that the hysteresis loop is very narrow and the difference between curves $O\ M\ G$ and $O\ K\ G$ is usually negligible. Furthermore, the important energy transformations occur only in that part of the cycle during which the flux is decreasing, so that for the present we shall ignore the part $O\ M\ G$ of the curve.

In the high-tension or "jump-spark" systems with which we are concerned the flux in the core is linked with both a primary and a secondary winding. The direct way to describe such a system would be to use two diagrams, one of which would show primary linkages plotted against primary current and the other secondary linkages plotted against secondary current. The first could be used

to trace transformations occurring while the secondary circuit was open and the primary circuit was acting alone (for example, periods 1 and 6 of the magneto cycle). The second graph would trace transformations occurring while the primary was open (for example, period 4). It is, however, more convenient and useful to combine these two diagrams by the artifice of plotting the secondary data on the same axes as the primary data, using as abscissas $n\ I_2$ and for ordinates $\frac{N_2\phi_2}{n}$ where n is a factor approximately equal to the ratio of secondary to primary turns. (See Appendix B for exact definition.)

The graph of secondary flux turns thus obtained still satisfies the important requirement that areas between any curve and the axis of ordinates represent energy transformed, since the ordinates have been decreased in the same ratio as that by which the abscissas have been increased.

It may also be shown (see Appendix B) that the secondary graph thus obtained will precisely coincide with the primary graph even if the coupling is loose, provided only that the ratio n (as defined by equation (7B)) is truly a constant and does not vary when measured at different flux densities and that current is flowing in one circuit only. Experimental confirmation of this result is shown in Figure 2. This gives the $N\phi$–I curve for a spark coil. The crosses were obtained from measurements of primary flux turns and primary current and the circles from similar measurements on the secondary. If the coupling is close (as is always the case in ignition apparatus), this coincidence also holds with sufficient accuracy for those parts of the cycle during which current is flowing in both circuits if the abscissas are taken as $I_1 + n\ I_2$.

We may, therefore, return to Figure 1 and trace the energy changes during the entire cycle, regarding the single curve $O\ K\ G$ as representing either primary or secondary quantities, provided the factor n is properly introduced. After the contact points close the primary current increases to the value $O\ B$ and the flux turns increase along the curve $O\ M\ G$ to the value $B\ G$. The energy then available is $H\ G\ K\ O$. The breaker points then open and period 2 begins. During this period currents flow in both primary and secondary windings charging the condensers associated with them. Theoretically these changes also might be traced on the $N\phi$–I diagram, but the net effect is that a certain amount of energy given by[1]

$$W_c = \tfrac{1}{2} C_o v^2 \tag{4}$$

is abstracted from the system. This is first stored in the condensers and then during period 3 is dissipated as heat in the spark gap

[1] For significance of symbols see notation listed on p. 674.

during the first or capacitance component of the spark. At the beginning of period 4, therefore, the system is represented by some point such as K. The energy W_c is represented by the area $H\ G\ K\ P$ and the remaining energy $P\ K\ O$ is dissipated later during period 4 in the inductive component of the spark. The secondary current in the spark at the beginning of period 4 is given by $\frac{PK}{n}$. Since

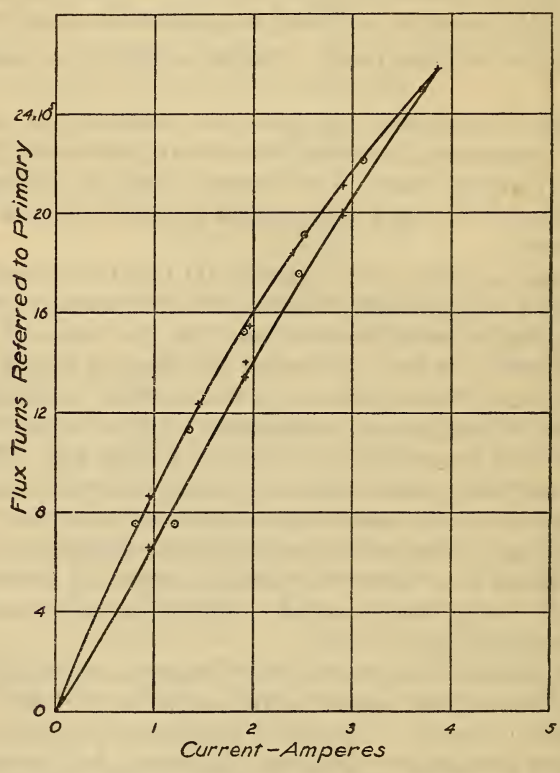

FIG. 2.—*Flux-turn current diagram for an ignition coil*

Abscissas are either primary current or secondary current times n. Ordinates are either primary flux turns or secondary flux turns divided by n. +'s indicate values measured on the primary. O's indicate values measured on the secondary.

the voltage required to sustain the spark during period 4 is roughly constant, $\frac{dN_2\Phi_2}{dt}$ is also constant and equal to $V_s \times 10^8$ lines per second. Hence, the flux drops linearly with time, and since the spark must cease when the flux has fallen to zero its duration is given roughly by

$$t = \frac{n\ P\ O \times 10^{-8}}{V_s} \text{ secs.} \tag{5}$$

Here V_s is the value of the voltage across the spark gap, and $P\ O$ is expressed in maxwell turns. The factor n enters if $P\ O$ is the primary flux turns while V_s is a voltage on the secondary.

The usefulness of the $N\phi$–I diagram becomes more evident when we consider its application to a magneto. Here the flux linking the coil depends not only on the current in the coil, but also on another variable—the angular position of the rotor with respect to the

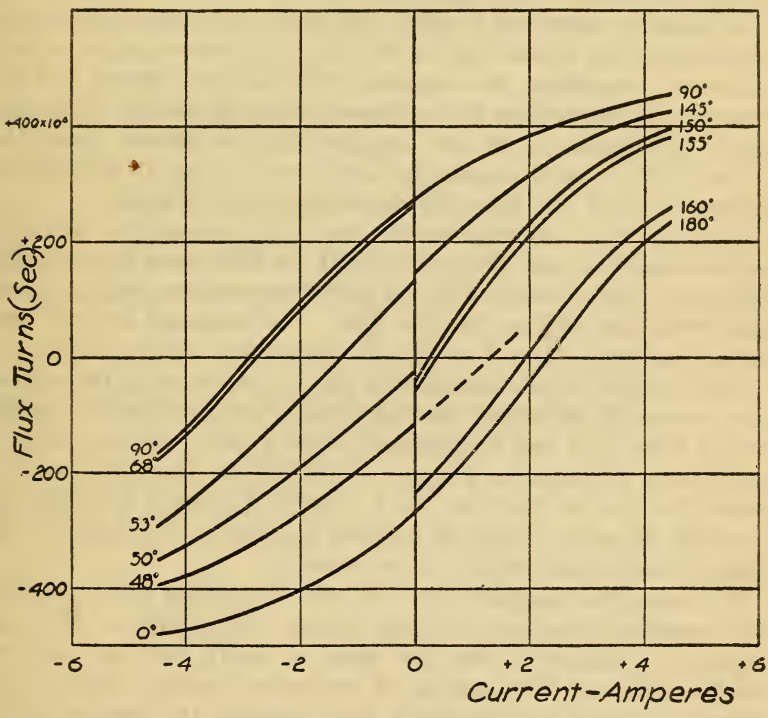

FIG. 3.—*Graphs of flux turns v. current for various angular positions of the rotor of a sleeve-type magneto*

Abscissas are primary currents. Ordinates are secondary linkages in maxwell turns

stator. To describe the purely magnetic characteristics we must use instead of the single curve $O\ K\ G$ of Figure 1, a family of curves each of which shows the relationship between flux turns and current for some particular angle. Such a diagram is shown in Figure 3 for a sleeve-type magneto which gives four flux reversals per revolution. It will be noted that each curve shows a flattening out at both ends as a result of magnetic saturation, and that the points of inflection lie roughly along the axis of abscissa where the flux is zero. The curves are somewhat similar in shape, since the principal

effect of rotation is to introduce more or less magnetomotive force from the permanent magnet into the magnetic circuit through the coil. However, rotation also changes the shape of the magnetic circuit considerably, so that the curves are by no means identical.

The curves marked 0°, 90°, and 180° correspond to rotor positions which give maximum values of flux through the coil. The curve for 90° is drawn for both directions of current. At this angle positive currents aid the permanent magnets. The other curves might also be extended to show the effect of reversed currents as suggested by the dotted line for 48°, but such extensions are of little value and complicate the diagram. For machines giving two flux reversals per revolution the continuous curve at the top of the diagram corresponds to the 180° position and the bottom curve (for 0° and 360°) is also necessarily continuous. If such machines are symmetrical, the two halves of the diagram will be alike.

In the case of magnetos having four flux reversals the curves do not necessarily repeat themselves until the 360° have been covered. However, if the armature and pole pieces are symmetrical, the second half revolution will be like the first. The alternate quarter revolutions (as can be seen from fig. 3) will usually not be alike.

The ordinate of the intersection of each curve with the axis of zero current is, of course, the flux linkage produced by the magnet acting alone and can be obtained from a curve of flux turns *v.* angle as is indicated in Figure 8. (It follows from the shape of these $N\phi$–θ curves that the $N\phi$–I curves, if plotted for equal increments of angle, would be bunched together at the edges of the diagram and spread widely in the center.)

In tracing the magneto cycle on such a diagram let us consider the somewhat idealized diagram shown in Figure 4. We may assume for simplicity that the speed is fairly low and that the breaker closes at the position of maximum flux *C*. Now, if the primary winding had absolutely zero resistance the rotation of the armature would generate enough primary current to maintain these linkages and after 180° rotation point *B* would be reached. The primary current would then be *O T* and the energy available for a spark would be the area *C B A*. Because of the primary resistance, however, the current generated in an actual machine will be less and the point representing the condition of the system will trace out a curve such as *C F D*. The energy now available for producing a spark is only *U D A* and the primary current is *U D*. The area *C D U* represents work done by the magnetic field in sending current through the primary resistance ($W=\int I_1^2R_1dt$), and which has been dissipated as heat in the winding; while the area *C B D* represents the difference between the work done by the prime mover driving

the magneto and the work which the prime mover would have had to perform if the primary resistance had been zero.

In the more usual case, the breaker is set to open the primary circuit and produce the spark before the rotor has turned the full 180° from the position of maximum flux. If the curve *F M P* corresponds to the angle at which break occurs, the state point is at *F* at the end of period 1. The energy lost as primary $I^2 R$ heat is only *C F E*, and the primary current at break is *E F*. Since periods 2 and 3 occupy such a very short time interval (at most 0.0005 second)

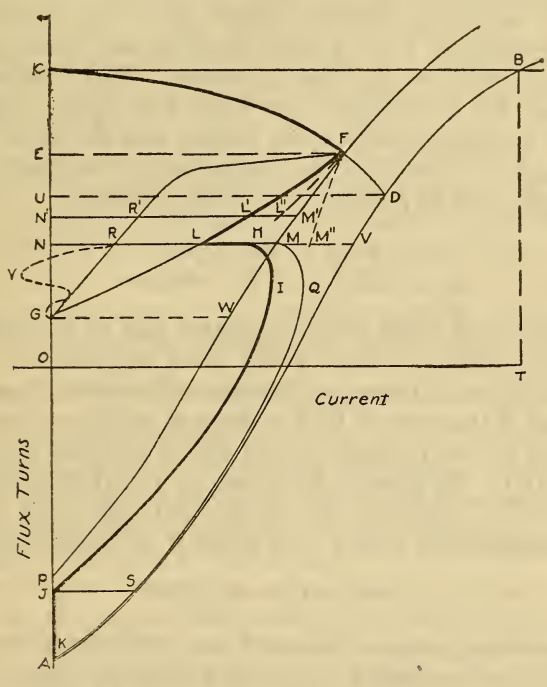

FIG. 4.—*Idealized flux-turn current diagram showing loci of state point under various conditions*

the rotor does not have time to move appreciably during these periods and the energy available without rotation is only *E F P*.

During period 2 of the cycle we have acting on the magnetic circuit the magnetomotive forces caused by three different currents which are flowing in the primary, secondary, and eddy current circuits, respectively. The exact variation of these currents with time is difficult to compute except on the basis of certain simplified model circuits like those discussed in Bureau of Standards Scientific Paper No. 424. (See also Appendix C.) In general, however, at any instant during period 2, as for example, when the flux turns are

given by $O\ N'$, the corresponding total magnetizing current $N'\ M'$ may be divided into a primary component $N'\ R' = i_1$, a secondary component $R'\ L' = n\ i_2$ and an eddy current component $L'\ M' = k_e\ i_e$ where i_e is the instantaneous value of the eddy current referred to the primary side. With the progress of the cycle the points of division R' and L' will trace out paths on the diagram while the point M' follows the locus $F\ M\ P$.

At the beginning of period 2 the total magnetomotive force results from the primary current $E\ F$ only. The transfer of current from primary to secondary, however, takes place very rapidly because of the close coupling which always exists between these two circuits in the usual forms of ignition apparatus. This transfer may be accompanied by oscillations,[2] but these are highly damped, and as a rough approximation we may assume that the locus $F\ R'\ R\ G$ of the primary current has the general shape indicated in Figure 4 and that the ratio of primary to secondary current,

$$\frac{N'\ R'}{R'\ L'} = \frac{N R}{R L} = \frac{C_1}{n^2 C_2} \tag{6}$$

does not vary very much over the greater part of the length of the curve. This relation is what would result according to the model circuit of Figure 11, Bureau of Standards Scientific Paper No. 424.

The trend of the curve $F\ L'\ L\ G$ depends entirely on the constants k_e and T_e of the eddy-current circuit and is discussed in more detail in Appendix C. In general, for values of T_e, which are large compared to $\sqrt{L\ C_0}$ (which is the usual case), this locus is approximately a straight line from F to a point G so located that

$$P\ G = (1 - k^2_e)\ P\ E \tag{7}$$

If the sparking voltage of the spark gap connected to the secondary is sufficiently low, a spark will occur at some stage in the process, say, when the flux turns are represented by $O\ N$. At this instant which marks the end of period 2 the primary current is $N\ R$, the secondary current is $\frac{R L}{n}$, and the eddy current referred to the primary circuit is $\frac{L M}{k_e}$. The energy which has been stored in electrostatic form in the primary condenser during period 2 is given by the area $E\ F\ R'\ R\ N$. The energy which has been stored in the secondary capacitance is given by the area $F\ L'\ L\ R\ R'$. The area $F\ M'\ M\ L\ L'$ represents the energy which has been made permanently unavailable by the eddy currents. Part of this energy has already been dissi-

[2] B. S. Sci. Paper No. 424, Figures 3 and 5. Also Appendix C of this paper.

pated as heat by the eddy currents during period 2. The remainder is stored in the leakage flux produced by the eddy currents and is dissipated as heat when the eddy currents die out later. (See Appendix C.)

Period 3 is a transition stage during which three rapid processes of readjustment occur as a result of the establishment of a conducting path across the spark gap.

These processes are (1) the discharge of the secondary capacitance into the spark gap, (2) the discharge of the energy of the primary condenser through the slight leakage inductance between primary and secondary windings and the transfer to the secondary winding of the ampere turns formerly maintained by the primary current, and (3) the rapid decrease of the eddy currents and the transfer of most of their ampere turns to the secondary winding. All these processes take place with exceeding rapidity but leave the magnetomotive force applied to the main core unchanged, while the general slow decrease in flux is determined by the relatively large time constant of the circuit composed of the total secondary inductance in series with the resistance of the secondary winding and spark gap. The result is that the flux turns do not change appreciably during period 3, and that $\frac{NH}{n}$, which is somewhat less than $\frac{NM}{n}$, represents the value of secondary current flowing at the end of period 3 and the beginning of period 4. The energy dissipated in the spark during period 3 and sometimes referred to as the "static component" of the spark is represented (neglecting a small amount of $I^2 R$ loss in the windings) by the area $E\ F\ L'\ L\ R\ N$.

If the spark gap is very long or the speed very slow so that the rotor does not move appreciably during the passage of the inductive component of the spark, and if there are no eddy currents, the state point during period 4 will move along the curve $M\ P$ and the energy dissipated in the spark gap will be $N\ M\ P$. After the spark ceases rotation on open circuit will gradually shift the state point from P to A during period 6.

Actually the rotor usually moves through an appreciable angle during the passage of the spark, so that the state point moves along some curve, such as $M\ Q\ S\ K$, which may or may not show an actual increase in secondary current between M and Q. The heat developed in the inductive component of the spark in this case is $N\ M\ Q\ K$. The excess of this over the area $N\ M\ P$ and the corresponding excess of current at each instant over that occurring in the absence of rotation are often referred to as the part of the heat or current due to the "rotational" or "generated" emf. There is, however, no fundamental difference between this excess area $M\ Q\ S\ K\ P$ and the

area $N\ M\ P$. An upper limit to the magnitude of this "rotational energy" is set by the area $M\ V\ A\ P$ since the flux turns can not increase above the value $O\ N$ unless an external emf is present in the secondary circuit.

As explained in more detail in Appendix C, the eddy currents do not entirely die out during period 3, so that the state point shifts from L to H and not to M during this period. As period 4 progresses the magnetomotive force of the eddy currents tends to increase as shown by the increasing distance between the curve $H\ I\ J$ and $M\ Q\ K$.

We therefore have the secondary current decreasing from I to J, while an eddy current builds up to a final value $\frac{J\ S}{k_e}$, which exerts enough magnetomotive force in the main core to keep the flux turns at the value $O\ J$ even though the secondary current has ceased entirely. As the rotation of the armature continues the eddy currents die out gradually, and at low speeds will fall to zero at K usually before the armature reaches the position corresponding to maximum flux at A.

The voltage across the secondary terminals is at any instant equal to

$$v_2 = \sqrt{\frac{2W_2}{C_2}} \tag{8}$$

where W_2 is the energy stored in the secondary condenser (C_2) at that instant. In the diagram this energy is represented by the area $F\ L'\ R'$. During period 2 as the line $N'\ R'\ L'\ M'$ moves downward this area and hence the secondary voltage increases rapidly at first and then more slowly until a maximum is reached when the flux turns have the value $O\ G$. If this maximum voltage does not exceed the sparking voltage of the spark plug, the spark gap will not break down and no spark will occur. Beyond this point the voltage begins to decrease, and the currents in the windings reverse their directions as energy flows out of the condensers and back into the magnetic circuit. The oscillations decrease progressively in amplitude as a result of the dissipation of energy in the resistance, and particularly in the eddy-current circuit, so that the system ultimately settles down to point P. However, we are not interested in tracing events beyond point G, since no spark will be produced after the system passes this point. This consideration emphasizes the important rôle played by eddy currents in injuring the performance of magnetos. Although the actual energy lost in the eddy-current circuit is the small area $F\ M'\ M\ L\ L'$, which in the limit when the magneto can just fire is $F\ M\ W\ G\ L$; yet the presence of the eddy currents renders the additional and very much

larger amount of energy $G\ W\ P$ unavailable for the production of voltage. On the reasonable assumptions that the lines $F\ G$ and $F\ P$ are straight and that $k^2_e=0.6$, 60 per cent of the original energy $E\ F\ P$ is rendered unavailable by a current which actually dissipates only 24 per cent of the energy.

III. METHODS FOR PLOTTING

The preceding paragraphs have indicated how the flux-turn-current diagram can serve qualitatively to represent the entire cycle of operations of a magneto or spark coil. To plot such diagrams quantitatively, data of three rather distinct types may be used. The first type of data is obtained by a flux meter or equivalent apparatus and serves to locate the family of curves showing the variation of flux turns with current for various constant angular positions of the magneto rotor. Such curves are shown in Figure 3. These curves serve to describe quantitatively the magnetic characteristics of the apparatus and fix upper limits to the possible values of current and energy delivered by it. The second type of data is obtained by oscillographic records of the primary and secondary currents and of the voltage across the breaker during a spark cycle. This type of data permits the plotting of the path of the state point for the particular conditions under which the oscillogram was taken. The changes of flux and current during periods 2 and 3 are so rapid, however, that the oscillograph fails to record them. Recourse must, therefore, be had to the third type of data, such as measurements of crest voltage, effective capacitance of the windings, and of the constants of the eddy-current circuits. Such data can then be fitted into one or another of the possible simplified model circuits and used to compute a probable locus for the state point during periods 2 and 3.

To obtain the first set of data, it is usually most convenient to use a flux meter or ballistic galvanometer which is connected to the secondary winding while a suitably controlled current is sent through the primary winding. The change in flux turns when a change is made in the primary current or in the angular position of the rotor can then be read directly on the flux meter. The instrument can be calibrated by having the secondary winding of a standard mutual inductor connected permanently in series with it and noting the deflection corresponding to the reversal of a known current in the primary of the inductor. Observations obtained in this way are primarily indications of the mutual inductance of the two windings. To obtain the self-inductance values—that is, the linkages which would be produced in either winding by a current in it rather than in the other—it is necessary to multiply the results by n_s (the ratio

of secondary self-inductance to mutual inductance; see N. A. C. A. Report No. 58) to reduce the results to a basis of secondary turns, or else to divide the results by n_p (the ratio of mutual inductance to primary self-inductance) to reduce them to a basis of primary turns. These ratios, as well as the mean ratio $n=\sqrt{n_s n_p}$ for use in translating between primary and secondary coordinates, can be obtained very conveniently by the procedure described in N. A. C. A. Report No. 58, Part II.

The presence of hysteresis in the magnetic circuit complicates the experimental procedure considerably. The method of observation indicated by Figure 5, while not theoretically perfect, has been found to work satisfactorily in practice. In this figure *a* shows

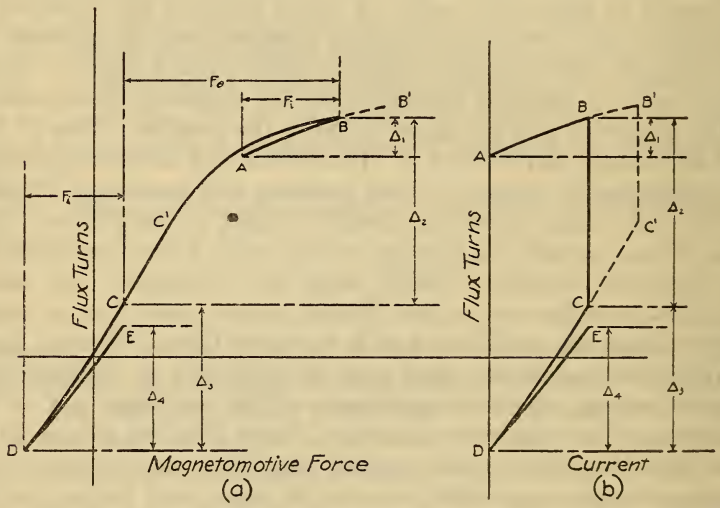

FIG. 5.—*Diagram illustrating procedure in obtaining graphs of flux turns v. current for fixed angular positions of a magneto rotor*

the flux turns as a function of the total magnetomotive force acting in the circuit while *b* shows the usual relation between flux turns and current. In this procedure the circuit is first brought into a cyclic state by repeated rotation or oscillation of the rotor between two extreme positions of maximum flux with no current flowing. The rotor is then clamped in one such maximum flux position corresponding to a point *A* in Figure 5. A current of the desired magnitude is then sent through the primary winding in such a direction as to aid the magnetomotive force of the magnets and bring the magnetic circuit to point *B*. In Figure 5 *a* the distance F_i represents the mmf due to the current. The change in flux turns resulting from the establishment of the current is observed on the flux meter and corresponds to Δ_1 in Figure 5. With the current still flowing

the rotor is turned through the desired angle θ. This moves the state point to C, where the distance $F\theta$ in Figure 5 *a* represents mmf introduced into the circuit by the permanent magnets, and Δ_2 gives the corresponding change in flux turns which is observed on the flux meter. The primary current is then interrupted, moving the state point to D and causing a change of flux turns Δ_3. If the circuit is again closed, the increase in flux turns Δ_4 is somewhat less than Δ_3 because of hysteresis.

To plot these data on the $N\phi$–I diagram Figure 5 *b*, points A and D are located from the curve of flux turns *v.* angle obtained on open circuit. Point C is then plotted at a distance Δ_3 above D and point B at a distance Δ_1 above A. By repeating this process with different values of current additional points, such as B' and C', can be located, thus fixing the curve. To obtain the curve for any other angle, it is merely necessary to repeat the process using a different angle of rotation between points B and C. The whole field may thus be mapped out in a family of curves. Points lying to the left of the axis of ordinates are obtained by starting at the next maximum flux point or by reversing the current instead of opening the circuit.

It will be noted from Figure 5 *b* that points C and D do not lie exactly on the normal hysteresis loop whose vertex is at A, but correspond to a loop starting at B. Since we are interested primarily in the difference Δ_3, the error introduced by the fact that both C and D lie a little above the true loop is quite negligible. The difference between Δ_3 and Δ_4 is also less than the maximum width of the normal hysteresis loop, but serves to give a rough check on the amount of hysteresis.

The summation $\Delta_2+\Delta_3-\Delta_1$ should, of course, be merely the difference in flux turns between A and D and should be independent of the value of current used in the measurements. The fact that this is experimentally found to be the case affords a convenient check on the measurements and justifies the neglect of the differences between the observed and true hysteresis loops.

Having obtained the family of $N\phi$–I curves for various angles by the methods described above, it is now possible from data of the second type to represent on this background the path of the state point during periods 1, 4, and 6 for any particular set of operating conditions (speed, gap voltage, etc.) for which an oscillogram is available. If the background curves have been obtained sufficiently close together, the plotting of a path consists merely in reading off from the oscillogram the various values of primary current corresponding to various angular positions of the rotor and plotting each on the appropriate curve (θ=constant) of the diagram.

If, however, only a few background curves are available, the path may still be plotted by applying the principle that the electromotive force induced in a winding is equal to the time rate of change of the flux turns; that is,

$$v = -\frac{d}{dt}N\phi \tag{9}$$

or

$$\Delta N\phi = -\int v dt \tag{10}$$

During period 1 the emf induced in the primary winding is used up in circulating the primary current through the resistance of the coil. We therefore have

$$v = R_1 i_1 \tag{11}$$

and

$$\Delta N_1 \phi_1 = -R_1 \int i_1 dt \tag{12}$$

where $\Delta N_1\phi_1$ is the change in primary flux turns between any two instants, R_1 is the primary resistance and i_1 is the value of the primary current at any instant. If the speed of the oscillograph film is f_s mm per second and the sensitivity of the current element with its shunt is f_a mm per ampere, then

$$\Delta N_1\phi_1 = \frac{R_1 a}{f_s f_a} \times 10^8 \tag{13}$$

where a is the area in square mm on the oscillogram bounded by the primary current record and its zero line, and by any pair of ordinates, while $\Delta N_1\phi_1$ is the change in primary flux turns between the instants corresponding to the same pair of ordinates.

During period 4 an oscillogram of secondary current gives the values of abscissas needed for the diagram, but (in the absence of a large number of background curves) the values of ordinate must be obtained from an independent but simultaneous record of the voltage across one of the windings. It is always much easier to measure this on the primary side; and if the resistance of the oscillograph vibrator circuit is kept at least as great as 200 ohms, it may be connected directly across the breaker contacts without materially interfering with the operation of the machine. While the breaker is open during period 4 this vibrator will give v_1 directly, and by equation (9) above, if f_v is the sensitivity of the voltage vibrator in mm per volt, we have

$$\Delta N_1\phi_1 = \frac{a}{f_s f_v} \times 10^8 \tag{14}$$

where a is the area in square mm on the oscillogram bounded by the primary voltage record and its zero line, and by any pair of

ordinates, while $\triangle N_1\phi_1$ is the change in primary flux turns between the instants corresponding to the same pair of ordinates.

The procedures indicated by equations (13) and (14) suffice to give only the changes in linkages between two points and not the actual value at any one point. If, however, any point is arbitrarily fixed as a base, the $N\phi$–I line can be plotted by combining the two procedures to give a continuous curve, extending from the beginning of period 4 to the end of period 1 of the succeeding cycle. During period 2 of each cycle, however, there is a break in the curve resulting from the very high value of voltage, and hence of rate of change of flux, which exists for a time interval so short that it can not be measured with any accuracy on the oscillogram. To complete the diagram, either the gap may be bridged by using data of the third type and inserting reasonable constants into some assumed model circuit and computing the resulting flux changes; or else the curve can be located by fitting it to the "background" of constant-position curves at some one point. It will be noted from the typical diagrams shown in Figures 8, 9, 11, and 12 that the path of the state point must necessarily touch the extreme position curves at two points (B and B') and these are usually the most desirable points to take as bases in locating the curves. In the neighborhood of these points the location of the background curve is affected very little by errors in the angular position of the rotor or in locating the proper ordinate on the oscillogram. Of course, any other constant-position curve, such as that corresponding to "break," might be used to locate the diagram but the precision is then usually less.

During period 4 eddy currents are present to a greater or less extent. It is therefore not possible to locate the diagram directly by angular position and secondary current. Hence, the data given by equation (14) must be plotted backward from a base point fixed in period 6.

During period 2 the changes in current and voltage are so rapid as to defy measurement by any of the usual methods. The best that can be done toward a quantitative representation of the phenomena occurring is to fit some theoretical model to the electrical quantities which can be observed and to plot on the diagram the computed details of the process occurring in the model. Two principal cases arise according as the secondary terminals are insulated or are shunted by a conducting path. For these cases the approximations suggested in the following paragraphs may be of assistance.

The closed-coil model, which assumes that there is a closed circuit of time constant T_e coupled to the main circuit with a coefficient

of coupling k_e, forms a basis for representing logically on the diagram the effect of eddy currents by the locus $F\ L'\ L\ G$ (fig. 4). A detailed discussion of this model is given in Appendix C, and a rigorous determination of the locus $F\ L'\ L\ G$ can be obtained by plotting pairs of values of $N_1\phi_1$ and I_1+nI_2 as given by equations (25c) and (26c) for successive values of t.[3] The procedure shown in Figure 6 serves to fix the locus roughly, but well enough for many purposes, if k_e and T_e are given. The quantity $s_e=\sqrt{L_2C_0}/T_e$ is first computed. The family of curves at the left side of Figure 6

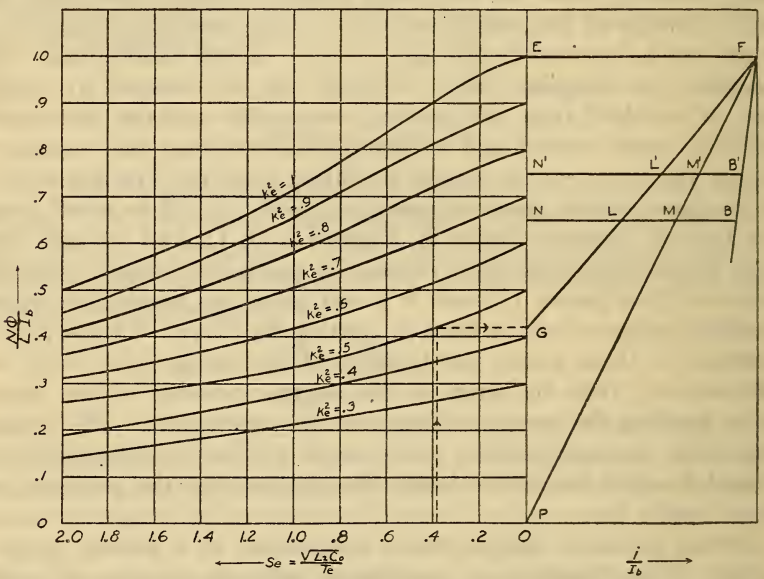

FIG. 6.—*Diagram for fixing the locus F G in plotting period 2 on the basis of a closed-coil model in which the eddy currents are assumed to flow in a circuit having constants* T_e *and* k_e^2. $s_e=\frac{\sqrt{L_2C_0}}{T_e}$.

then show for the given value of k_e^2 and the computed value of s_e, the height $P\ G$ of point G above point P on the $N\phi$—I diagram. The ordinates in Figure 6 are expressed as fractions of the total change in flux turns from F to P.

If, however, the crest voltage, which the system is just capable of delivering with the secondary circuit open, and the total effective capacitance C_0 are given, the locus can be assumed to be a

[3] Considerable justification for the use of the closed-coil model to represent the effect of eddy currents is found in the detailed analysis by Snow of the corresponding effects in an infinitely long circular core. It can be shown that the use of the first (and predominant) term of his series expansion is equivalent to the assumption of a single tertiary circuit of fixed time constant given by $T_e=\frac{\pi\mu D^2}{2.405\rho}$.

straight line situated so that the area $E\ F\ G$ (fig. 4 or fig. 6) is equal to the electrostatic energy $1/2\ C_0V_m^2$. This condition is satisfied when

$$EG = \Delta N\phi = \frac{C_0V_m^2}{I_1} \times 10^3 \tag{16}$$

A representation of the phenomena in an ignition system during period 2 is given in some respects more completely by the double-coil model. The equations of Taylor-Jones[4] and others enable a complete solution of the problem to be worked out, so that simultaneous values of i_1, i_2, $N_1\phi_1$, and $N_2\phi_2$ can be obtained and plotted. However, the diagram thus obtained is very complex and hence for many purposes hardly justifies the labor of constructing it.

Another important case arises when the secondary terminals of the ignition coil are not insulated as has been assumed in the preceding paragraphs, but are connected by a resistance S, which may be thought of as resulting from the presence of a conducting deposit of carbon on the surface of the spark-plug insulator. In this case the simplest model which approximates the actual conditions is obtained by neglecting the eddy currents and the secondary capacitance and regarding the system as a primary circuit, having the constants of the actual primary, coupled with a circuit having the inductance of the secondary and the resistance S (or more precisely $S+R_2$). The coupling between these circuits can not be assumed to be perfect but is in all practical cases so close that no distinction need be drawn between the linkage $N_1\phi_1$ and $\frac{N_2\phi_2}{n}$ in plotting the ordinates of loci on the diagram.

For such a pair of circuits the course of events during period 2 is completely described by plotting on the diagram the locus of the primary current i_1 for various values of $N_1\phi_1$. Such a plot is shown as $F\ R\ J\ D$ at the right side of Figure 7. It should be noted that in this model the secondary terminal voltage reaches its crest value when the secondary current is greatest, and hence when the primary current is near its maximum negative value and not at zero as is the case on open circuit. An exact representation on the basis of this model can be obtained by plotting pairs of values of $N_1\phi_1$ and i_1 as computed by equations (25c) and (26c) for a succession of values of t.

An approximate diagram can be obtained by sketching a curve of the general shape of $F\ R\ J\ D$ (fig. 7). This curve must leave point F with a horizontal tangent and must at point D be tangent

[4] E. Taylor-Jones, Phil. Mag., 22, p. 706, 1911; Phil. Mag., 27, p. 565, 1914; Phil. Mag., 29, p. 2, 1915; Phil. Mag., 30, p. 224, 1915; Phil. Mag., 36, p. 145, 1918; Electrician, 83, pp. 167–169, 201–202, 1919.

to a line (as $X\ Y$) which is parallel to the line $F\ P$. Point D can be located for given values of k^2 and S as follows: First, compute the quantity $s=\frac{S}{n^2}\sqrt{\frac{C_1}{L_1}}$; then, using the family of curves in the upper left corner of Figure 7, locate point D' on the curve (such as $A\ B$) corresponding to the given k^2 and s; draw the horizontal line $D'\ D$; the intersection of this with the corresponding curve $O\ C$ in the central family gives the point D desired.

The interpretation of a plot of $N_1\phi_1$ versus i_1 on this diagram is as follows: While the primary current is decreasing from its origi-

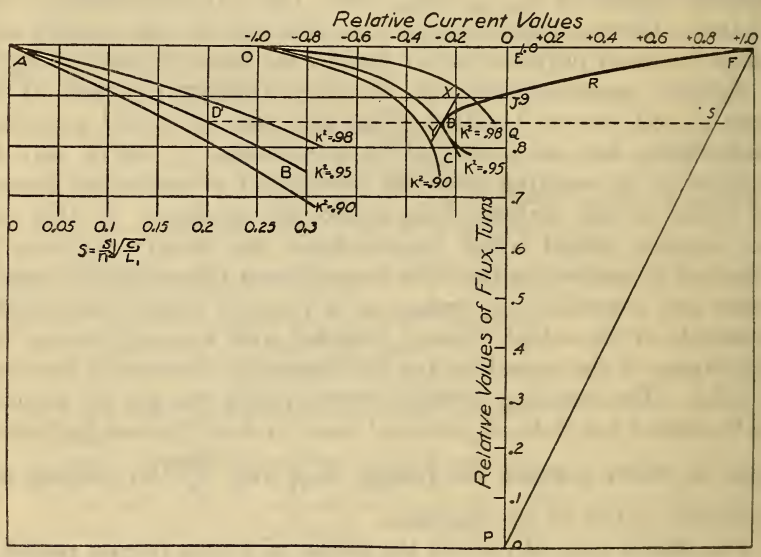

FIG. 7.—*Diagram for fixing the locus F J D in plotting period 2 on the basis of a two-coil model with the secondary condenser omitted and with a shunting resistance S across the secondary terminals*

nal value to zero it delivers to the primary condenser an amount of energy represented by the area $E\ F\ R\ J$ (fig. 7). After the primary current reverses energy begins to flow out of the condenser, and when a point such as D is reached the energy thus restored corresponds to the area $J\ Q\ D$. Meanwhile there has been a steady dissipation of energy in the shunting resistance connected to the secondary, and this is indicated approximately by the area $F\ S\ Q\ D\ J$.

The emf of rotation, which in the case of magnetos acts in all the circuits in addition to the voltages caused by induction-coil action, is usually negligible. Its effect can, if desired, be computed from the equations given in Appendix C. In general, it tends, as shown by the lines $F\ L''$ and $F\ M''$ in Figure 4, to make

the loci $F\ L$ and $F\ M$ slope downward from point F more steeply than they would in the absence of an emf. The small areas, such as $F\ M''\ M$, represent energy contributed directly by the prime mover during the rotation.

During the short transition period (3), which extends from the instant the spark gap breaks down to the time when the circuits have settled down to a state in which a steady current is flowing in the arc across the spark-plug points, two distinct events occur. The first event is the discharge of the secondary capacitance through the circuit consisting of the spark plug and its leads. This discharge may involve very high values of current, but since this current does not encircle the core it has no effect on the flux and hence none on the $N\phi$–I diagram. The second event is the shift of the electrical conditions in the windings from the current and voltage values existing just before the spark started to the new set of values characteristic of the steady arc state which exists during period 4. As is shown in Appendix C, this latter event causes oscillations of considerable magnitude and very high frequency to occur in both primary and secondary currents. However, the total flux in the core does not partake of these oscillations to an appreciable extent. The state point representing $i_1+n\ i_2$ which reaches point L (fig. 4) at the end of period 2 in effect moves horizontally to H as the eddy currents shift rapidly to the new value corresponding to the reduced rate of change of flux. It then follows along the curve $H\ I\ J$ during period 4. The oscillations started in period 3 may, perhaps, last well into period 4, and if desired can be represented by a locus of $N_2\phi_2$ plotted against i_1, as shown by the dotted line $R\ Y$ in Figure 4. There seems to be at present, however, little basis available for estimating their magnitude or damping quantitatively.

IV. TYPICAL DIAGRAMS

Figures 8, 9, 11, and 12 show examples of flux-turn current diagrams based on data obtained with a magneto of the usual shuttle-core type operating under four different conditions. In all cases the magneto was firing a set of four standard 3-point spark gaps, which had a spacing of 5 mm. In Figures 10 and 13 the oscillograms on which the diagrams are based have been replotted to uniform scales of current, voltage, and angle. In the diagrams the heavy line represents the path of the state point; the lighter lines are the "background curves" obtained by flux-meter measurements. One of the coordinate squares corresponds to 1 ampere and 4×10^6 linkages and hence to 0.04 joules. The letters distributed along the curves serve to correlate corresponding points on the diagrams and oscillograms.

The right half of Figure 8 shows the linkage-current diagram for this magneto at 100 r. p. m. at full advance and was derived from the oscillogram shown in Figure 10 *a*. It will be noted that a very appreciable amount of energy indicated by the area *A B C F E* is dissipated in the resistance of the primary winding. The energy *E F H J* in the spark is moderate, and the path is nearly straight from *H* to *J* because the low speed produces little emf of rotation. The small negative loops appear because the breaker closes before the flux has reached its maximum value.

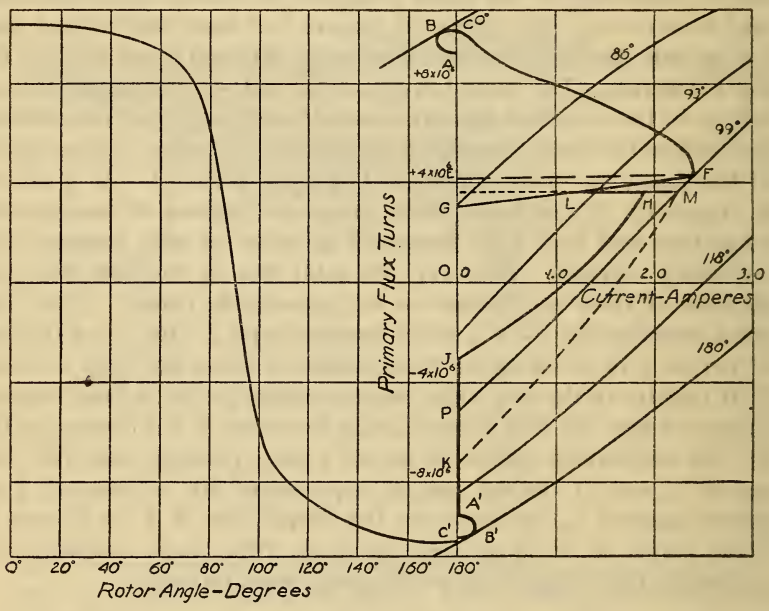

FIG. 8.—*Right side of figure is the Nφ-I diagram based on oscillograms (fig. 10 a) taken on a shuttle-core magneto operating at 100 r. p. m. full advance. Left side of figure is a graph of flux turns v. angular position for the same magneto with no current flowing*

The left half of the figure is a plot of open-circuit flux against angle for one-half rotation of the armature and serves to locate the lower ends of the family of background curves.

Figure 9 was drawn from data obtained at 100 r. p. m. full retard (See fig. 10 *b*.) The great effect of primary resistance is even more marked here. The energy available at break *E F P* is small, and at this speed sparking was irregular. The later closing of the breaker has eliminated the negative loop.

Figure 11 was obtained with the magneto at 1,000 r. p. m. full retard and brings out the effects of speed. The oscillograms on which it is based are shown in Figure 13 *a*. The $I^2_1 R_1$ loss from *A* to *E* is relatively small. From *E* to *F* an arc persisted across the

breaker contacts while the current dropped from 5.1 to 4.0 amperes. The arc then broke and the spark was produced. The energy loss resulting from the arcing is indicated by the area *X E F Y*. The secondary current died out at *J* before the breaker closed, and because of the late timing the emf of rotation contributed but little to the spark energy. During the latter part of period 4 the eddy currents built up to a considerable magnitude, and their decay after the spark ceased is indicated in the voltage wave (fig. 13 between *J* and *A′*). When the breaker closed at *A′*, the eddy-current

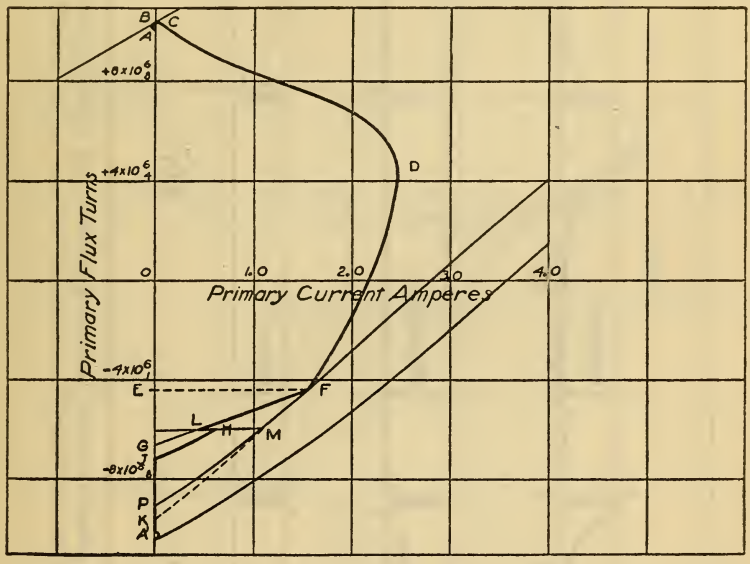

FIG. 9.—*Nφ-I diagram for the shuttle-core magneto based on oscillograms (fig. 10 a) taken at 100 r. p. m. full retard*

energy is transferred to the primary circuit and builds up the large negative loop at *B′*.

Figure 12 is based on oscillograms (fig. 13 *b*) taken at 2,500 r. p. m. full advance and is drawn to show two successive sparks. The speed is now so great that the effects of primary resistance have almost vanished and the state point moves from *B* to *F* at practically constant flux turns. The emf due to rotation is very effective and raises the secondary current from *H* to a maximum at *I*, contributing the energy indicated by *H I A′ Q* to the spark. Another result of the high speed is that the breaker closes at *A′* while the current in the spark is still very considerable.

The current through the spark then dies out with great rapidity while the primary current builds up correspondingly. As the eddy

currents die out from A' to B' the primary current increases still further and then starts to reverse under the influence of the emf due to rotation which is now in the opposite direction. The flux-turn current diagram for the next spark is of substantially the same shape but has smaller values of current. It will be noted that the

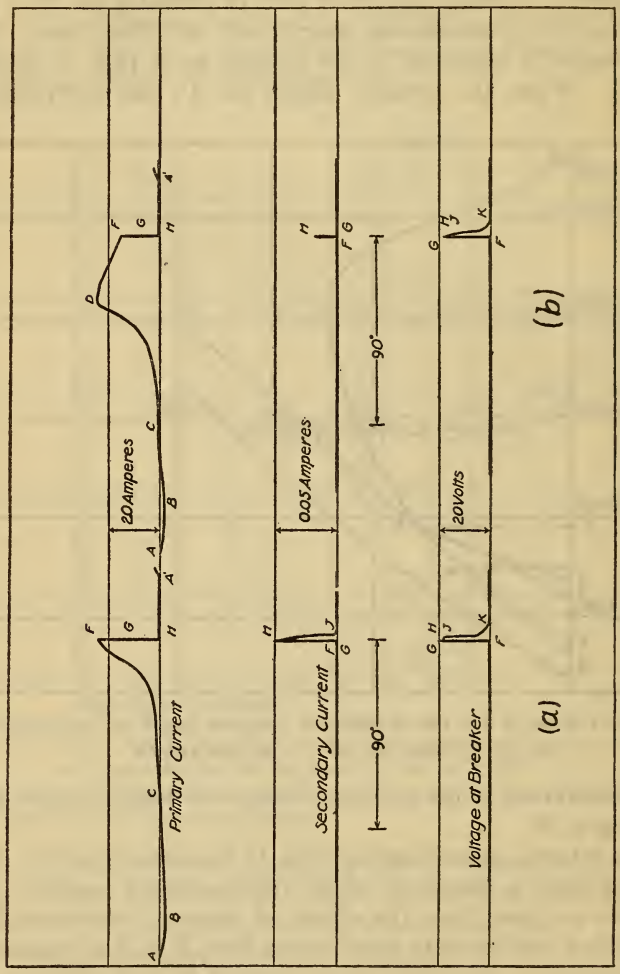

FIG. 10.—*Oscillograms of primary current, secondary current, and voltage across the breaker contacts; taken with shuttle-core magneto operating at 100 r. p. m. (a) at full advance and (b) at full retard*

closed curve traversed by the state point during two successive sparks must necessarily lie between the limiting curves for $\theta=0°$ and $\theta=180°$ and be tangent to these at points such as B and B'. The loop may, however, be shifted up or down so as to become quite unsymmetrical. In extreme cases this shift leads to a condition where misfiring occurs persistently on alternate sparks.

In plotting Figures 8, 9, 11, and 12 the cycle diagrams have been located by the points of tangency with the $\theta=0°$ and $\theta=180°$ curves. All errors of measurement are thereby accumulated in the narrow margin between F and H and hence give a somewhat misleading impression of the energy changes in periods 2 and 3. The oscillograms on which the diagrams were based were originally taken for a quite different purpose with the result that their accuracy, particularly that of the wave of primary voltage, is rather poor.

The energy exchanges during these periods are, however, indicated in Figures 8 and 9. In the former diagram data was available

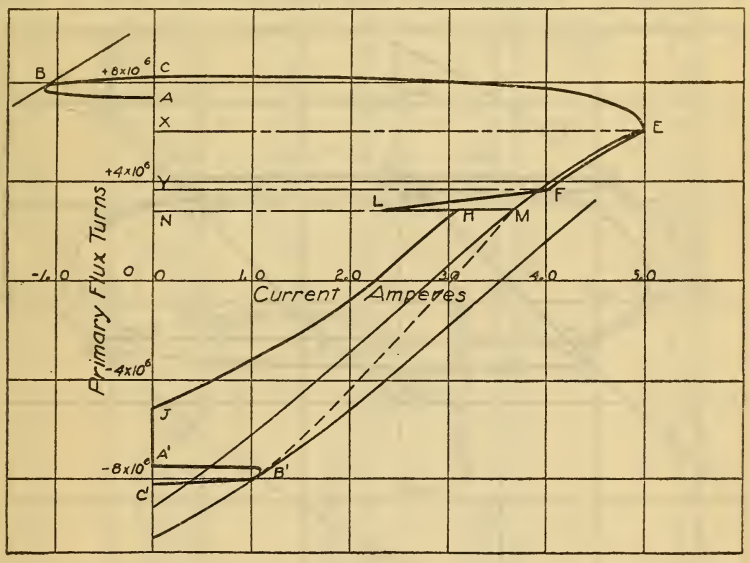

FIG. 11.—*Nφ-I diagram of the shuttle-core magneto based on oscillograms (fig. 13 a) taken at 1,000 r. p. m. full retard*

An arc persisted across the breaker contacts from E to F

on the maximum voltage attained when no spark gap was connected to the secondary and the locus $F\ L\ G$ was located by the method suggested on page 665. In the latter diagram locus $F\ L\ G$ is fixed by the method given in Figure 6, using values of k_e and T_e for the eddy current circuit observed with 3,000-cycle alternating current.

A noticeable feature of all the diagrams is the fact that the path of the state point during period 4 lies at smaller secondary current values than correspond to a line of constant angle drawn through the primary current value at the instant of break. While part of this displacement may be the result of experimental error, there seems to be a very definite indication that the main cause of the displacement is the presence of eddy currents. Since the effect of such currents is

to add a magnetomotive force proportional to $k_e\ i_e$, the dotted lines $M\ K$ or $M\ B'$ are sketched in to suggest, by their horizontal distance from the solid curve $H\ J$ *or* $H\ A'$, the probable magnitude of this effect.

An alternative but less probable explanation of the displacement can be made by assuming that the energy required for the production of a spark is materially greater than that represented by the energy stored in the condenser. On this basis points H and J in Figures 8, 9, and 11 and the curve joining them would then be plotted lower, so that, for instance, H would be on the curve of θ=constant passing through F. The change in flux turns between J and A' would,

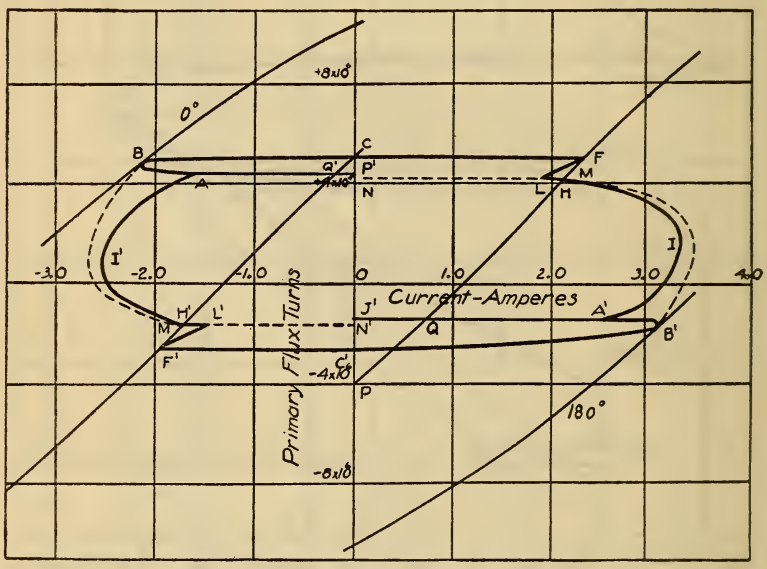

FIG. 12.—*Nφ–I diagram of the shuttle-core magneto based on oscillograms (fig. 13 b) taken at 2,500 r. p. m. full advance. Path is plotted for two successive sparks*

of course, be correspondingly reduced, but not by more than could, perhaps, be attributed to observational errors. The eddy-current values resulting from the alternative assumption are in slightly better agreement with those deduced from the observations made with 3,000-cycle alternating current. On the other hand, the assumption requires that the postulated energy be forced into the spark gap by a current which can not exceed I_b/n at a voltage which can not exceed the sparking voltage of the gap. The time required to transmit the postulated energy at this current and voltage while short is long enough to be almost appreciable on the oscillogram, yet the photographic record shows little, if any, indication of such a time interval.

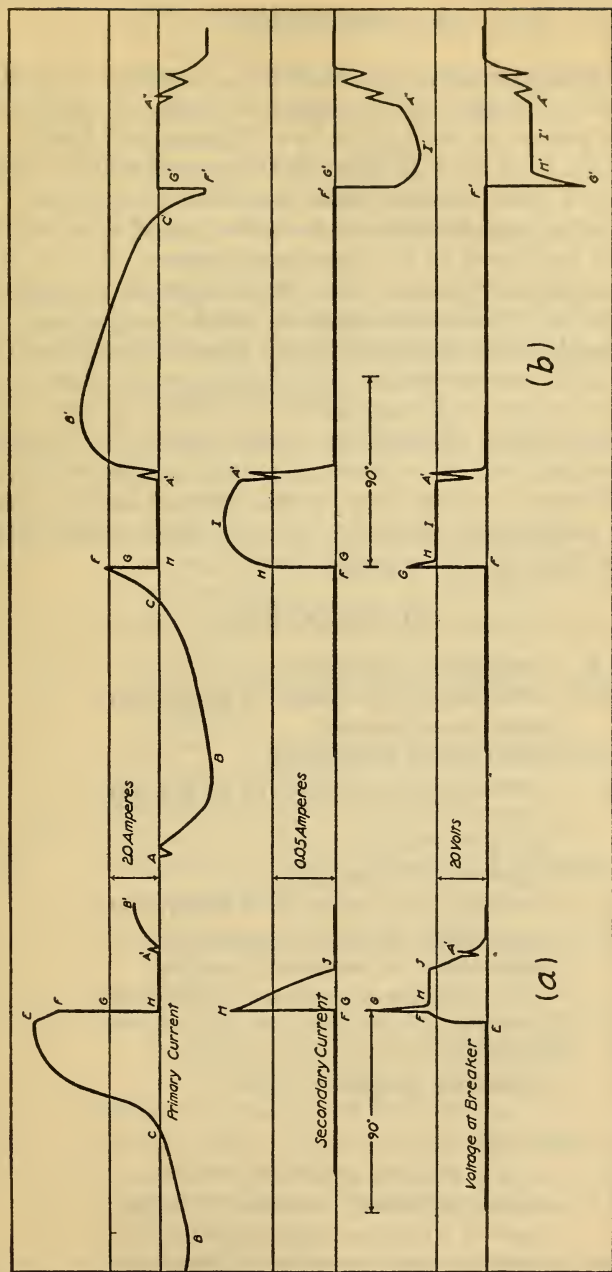

FIG. 13.—*Oscillograms of primary current, secondary current, and voltage across the breaker contacts; taken with shuttle-core magneto operating at (a) 1,000 r. p. m. full retard and (b) 2,500 r. p. m. full advance*

V. CONCLUSIONS

The foregoing discussion has set forth a procedure for analyzing the electrical performance of a magneto or spark coil and for representing the process occurring in it in a diagrammatic fashion. The four examples given serve to illustrate the general shape of diagram to be expected under the more usual conditions of operation. They also serve as an experimental check on the general applicability of the method by reason of the agreement between the two sets of data obtained by the flux meter and the oscillograph, respectively.

The precision of the measurements on which the diagram is based can doubtless be made materially higher than in the present experiments, in which case the method should give a rather direct and useful basis for estimating the magnitude and effects of eddy currents.

Even in the absence of quantitative data, however, it is hoped that the diagram may still prove useful in purely qualitative discussions of the phenomena concerned and of the effect of various operating conditions on these phenomena. It is for this latter purpose that the main value of applying it to periods 2 and 3 lies.

VI. NOTATION

A, A', A_2, A_e	= constants of integration.
A_{11}, A_{12}, etc.	= coefficients in constants of integration.
a	= area on oscillogram.
B, B', B_2, B_e	= constants of integration.
B_{11}, B_{12}, etc.	= coefficients in constants of integration.
b	$=\frac{r+s}{3(1-k^2)}$.
C, C'	= constant of integration.
C_{11}, C_{12}, etc.	= coefficients in constants of integration.
C_1	= capacitance of primary condenser.
C_2	= capacitance of secondary winding.
C_o	= total effective capacitance of windings.
c	$=\frac{r\,s+1}{3\,(1-k^2)}$.
D	= Diameter of core.
d	$=\frac{s}{1-k^2}$.
E_1	= emf in primary caused by rotation.
E_2	= emf in secondary caused by rotation.
e	= base of Napierian logarithms = 2.718.
F_{11}, F_{12}, etc	= coefficients in constants of integration.
f_a	= current sensitivity of oscillograph vibrator mm per ampere.
f_s	= speed of oscillograph film, mm. per second.

f_v	= voltage sensitivity of oscillograph vibrator mm per volt.
G_{11}, G_{12}, etc.	= coefficients in constants of integration.
H_{11}, H_{12}, etc.	= coefficients in constants of integration.
I	= currrent.
I_b	= primary current at break.
I_e	= initial value of eddy current.
I_1, I_2	= initial values of primary and secondary currents, respectively.
$(I_e)_1$, $(I_e)_2$	= value of eddy current at $t=t_1$, $t=t_2$, etc.
i, i_e, i_1, i_2	= instantaneous values of currents.
k	= coefficient of coupling between primary and secondary windings $=\sqrt{\frac{M^2}{L_1 L_2}}$.
k_e	= coefficient of coupling between secondary and eddy current circuits.
L	= self-inductance.
L', L''	= "equivalent" or "effective" inductance.
L_1, L_2	= inductance of primary and secondary circuits, respectively.
l_1, l_2	= flux leakage factors of primary and secondary circuits.
M	= mutual inductance between primary and secondary circuits.
M_e	= mutual inductance between secondary and eddy current circuits.
m	= variable in auxiliary equation.
m_1, m_2, m_3	= roots of auxiliary equation.
N_1, N_2	= number of turns in primary and secondary windings, respectively.
n	= effective ratio of turns $=\sqrt{\frac{L_2}{L_1}}=\sqrt{n_s n_p}=\frac{N_2}{N_1}$ approximately.
n_p, n_s, n_m	= turn ratio as observed by changing flux in primary, secondary, and magnet, respectively. (See N. A. C. A. Report No. 58.)
P	= instantaneous power in circuit.
P_1, P_2	= mutual flux per ampere turn in primary and secondary, respectively.
q	$=mT$ = variable of auxiliary equation in dimensionless form.
q_1, q_2, q_3	$=m_1T$, m_2T, m_3T = roots of auxiliary equation in dimensionless form.
R_1, R_2, R_e	= resistances of primary, secondary, and eddy current circuits, respectively.

R'	= total effective resistance.
r	$=\frac{R_1}{L_1}T=R_1\sqrt{\frac{C_1}{L_1}}=\frac{R_1\ C_1}{T}$.
S	= resistance of shunting circuit across secondary terminals.
s	$=\frac{R_2}{L_2}T=\frac{T}{T_2}$.
s_e	$=\frac{R_e}{L_e}T=\frac{T}{T_e}$.
T	$=\sqrt{L_1\ C_1}$.
T_e, T_2	= time constants of eddy-current circuit and secondary circuit respectively, $\frac{L_e}{R_e}$, $\frac{L_2}{R_2}$.
t	= time.
u	$=\frac{T_e}{T_2}$.
V_m	= crest value of secondary voltage.
V_1, V_2	= initial or constant values of primary and secondary voltage, respectively.
V_g	= breakdown voltage of the spark gap.
V_s	= voltage required to sustain an arc at the spark gap.
v	= instantaneous voltage in any coil.
v_1, v_2	= instantaneous primary and secondary voltage.
W	= energy.
W_c	= energy in capacitance.
x, y	= typical variables.
α, β	= real and imaginary parts of m_2 and m_3.
δ, γ	= real and imaginary parts of q_2 and q_3.
θ	= angle of position of rotor.
λ_1, λ_2	= roots of auxiliary equation.
μ	= permeability.
ρ	= resistivity.
ϕ	= magnetic flux.
ϕ_1, ϕ_2	= flux linking primary and secondary, respectively.

VII. APPENDIXES

APPENDIX A. PROOF OF ENERGY RELATION

If we consider a coil of N turns which is linked by a flux ϕ, the electromotive force induced in it at any instant is given by

$$v=-N\frac{d\phi}{dt} \tag{1a}$$

where $\frac{d\phi}{dt}$ is the time rate of change of flux at that instant. If a current i is flowing in the coil at the same time, the power (rate of transfer of energy) in the circuit is

$$P=v\ i \tag{2a}$$

and the electrical work done between any two epochs t_1 and t_2 is

$$W=\int_{t_1}^{t_2}Pdt\int_{t_1}^{t_2}vidt=\int_{t_1}^{t_2}-iN\frac{d\phi}{dt}\,dt=-\int_{t_1}^{t_2}id(N\phi) \tag{3a}$$

The minus sign merely indicates that if the linkages are increased the induced electromotive force opposes a current which would of itself produce such linkages. For such an increase in linkages W represents the electrical work which has been supplied from without (perhaps by a battery) and has been stored in the magnetic field. Conversely, when the flux turns decrease during the interval, energy has left the magnetic field and has been transformed into the electrical work needed to assist in circulating the current i through the circuit. If the current is flowing in a closed metallic circuit, the electrical work all goes into heat produced in the resistance of the circuit. If a condenser is in series, the bulk of the work is used in charging the condenser and raising its voltage, while if a storage battery were in circuit, part of the electrical work might appear as chemical energy in the battery.

Now, in general, if a variable y is plotted as ordinate against another variable x as abscissa, the area between the resulting graph and the axis of ordinates is given by

$$a=\int_{y_1}^{y_2}xdy \tag{4a}$$

a comparison of equations (3a) and (4a) shows that if we plot $N\phi$ as ordinate against i as abscissa the area between the graph and the $N\phi$ axis will be proportional to the electrical work done by or on the circuit.

Since equation (3a) holds for any consistent system of units, it will give W in joules when i is in amperes and $N\phi$ is in units of 10^8 maxwell turns.

APPENDIX B. DEFINITIONS OF RATIO

The ratio of secondary to primary turns in an induction coil or magneto can be obtained exactly only by actual count, which is not usually practicable even by the manufacturer, since it is customary to wind the secondary with an amount of wire sufficient to fill a given space rather than to apply a given number of turns. The ratios of importance in the operation of the coil, however, are really ratios of the linkages or flux turns, since a turn which does not link flux might as well be absent as far as its effect on performance is concerned.

Part II of Report No. 58 N. A. C. A. contains a detailed description of an accurate and convenient method of measurement which gives this effective ratio. The ratio of secondary to primary flux turns, measured by varying or reversing a current in the primary winding, is there denoted by n_p. The slightly different ratio of flux turns observed when the core is magnetized by a current in the secondary is denoted by n_s. The intermediate value obtained by noting the ratio of the changes in flux turns of the two windings when the armature is rotated is denoted by n_m. In considering the relations between these various ratios we may note that the flux turns in a coil under given conditions can be represented as the product of several factors. Thus, in measurements with current in the primary we have

$$N_1\,\phi_1=N^2_1\,P_1\,(1+l_1)\,I_1 \tag{1b}$$

$$N_2\,\phi_2=N_1\,N_2\,P_1\,I_1 \tag{2b}$$

Here N_1 and N_2 are the actual numbers of primary and secondary turns while P_1 is the mutual flux resulting from a magnetomotive force of 1 ampere turn acting in the primary. This quantity will, of course, vary considerably with changes in I_1 and hence in flux density and permeability. The factor $(1+l_1)$ represents the magnetic leakage so that $P_1\ l_1$ is the additional primary leakage flux per ampere turn. l_1 is also a function of permeability, and will, in general, increase slightly with increase in I_1. Equation (1b) may be considered as the functional relation between $N_1\ \Phi_1$ and I_1 represented by the graphs on the $N\ \Phi$–I diagram. From equations (1b) and (2b) we see that

$$n_p = \frac{N_2 \phi_2}{N_1 \phi_1} = \frac{N_2}{N_1} \frac{1}{(1+l_1)} = \frac{M}{L_1} \tag{3b}$$

Similarly, when current is sent through the secondary only we have

$$N_2\ \phi_2 = N^2_2\ P_2\ (1+l_2)\ I_2 \tag{4b}$$

$$N_1\ \phi_1 = N_1\ N_2\ P_2\ I_2 \tag{5b}$$

and

$$n_s = \frac{N_2 \phi_2}{N_1 \phi_1} = \frac{N_2}{N_1}(1+l_2) = \frac{L_2}{M} \tag{6b}$$

Where l_2 represents the relative secondary leakage and will increase somewhat with increase in flux density.

Here L_1=primary self-inductance,
L_2=secondary self-inductance,
M =mutual inductance between primary and secondary.

It may also be noted that if the magnetic circuit be thought of as consisting of three parallel magnetic paths, one of which is common to both windings while each of the others is linked with one of the windings only, then P_1 or P_2 represents the reciprocal of the reluctance of the common circuit expressed in ampere turn units; and hence $P_1 = P_2$ provided conditions are such that the flux density in this common magnetic circuit is the same when n_s and n_p are determined.

It is evident, however (and this is borne out by experiment), that both n_p and n_s are much less dependent on flux density than either L_1, M, or L_2. Furthermore, n_p decreases while n_s increases with increase in flux density. If we therefore define a mean ratio

$$n = \sqrt{n_p n_s} = \frac{N_2}{N_1}\sqrt{\frac{1+l_2}{1+l_1}} = \sqrt{\frac{L_2}{L_1}} \tag{7b}$$

it is evident that n will be nearly constant for all conditions and will be a close approximation to the turn ratio $\frac{N_2}{N_1}$.

From (4b) and (7b) we see that

$$\frac{N_2 \phi_2}{n} = N_1^2 \frac{(1+l_2)}{\left(\frac{1+l_2}{1+l_1}\right)} n\, I_2\, P_2 \tag{8b}$$

Now, in equation (8b) P_2 l_1 and l_2 all depend on the flux density, but as shown above the ratio in the denominator is independent of flux density provided l_1 and l_2 correspond to the same flux density. The value of this ratio

will therefore be unaffected if we arbitrarily choose to regard the ratio as pertaining to the particular flux density actually produced by I_2. We may, therefore, cancel the factor $(1+l_2)$ and obtain

$$\left(\frac{N_2\phi_2}{n}\right)=N^2{}_1P_2(1+l_1)\ (nI_2) \tag{9b}$$

as the functional relation between $\frac{N_2\phi_2}{n}$ and $n\ I_2$ where P_2 and l_1 have values pertaining to the actual flux present in the core when the current is I_2. The quantities $\frac{N_2\phi_2}{n}$ and $n\ I_2$ may be considered as ordinate and abscissa of a second graph. A comparison of (9b) with (1b), which is the corresponding relation between the coordinates of the graph of primary quantities, shows that the equations are identical, since it has already been shown that $P_2=P_1$ for equal flux densities. The graph of secondary quantities as thus modified will, therefore, necessarily exactly coincide with the similar primary graph.

A single curve is therefore sufficient to show both the primary flux turns produced by primary current alone and the secondary flux turns produced by secondary current alone, and hence may be called the "self-inductance curve." A second curve, the ordinates of which were reduced in the ratio $1 : \sqrt{(1+l_1)\,(1+l_2)}$ or $n\ M : L_2$ as compared with the preceding, would serve to give the primary flux turns produced by a secondary current, and vice versa, and might be called the "mutual-inductance curve."

During period 1 of the cycle of operation current flows in the primary coil only, and during period 4 current flows in the secondary only. The state point moving on the self-inductance curve defined above, therefore, indicates the magnetic flux condition which is of importance during these two periods. An auxiliary state point moving on the mutual-inductance curve may, if desired, be used to represent the condition in the other circuit. During period 2, however, currents are present in both coils, and the self and mutual fluxes, if plotted as ordinates for values of I_1+nI_2 as abscissas, will fall at points between the two curves. If the coupling between the coils is loose, these two curves are well separated and the loci needed to properly describe the magnetic conditions become so complex as to neutralize the gain from combining the primary and secondary diagrams.

If, on the other hand, the coupling is very close, as is nearly always the case in ignition apparatus, the self- and mutual-inductance curves practically coincide, and a single state point on this common curve at an abscissa$=I_1+nI_2$ indicates correctly the flux produced by the combined magnetomotive forces of the two currents. The difference between the two curves is $(1-k)$ which in most ignition apparatus ranges from 0.09 to 0.01.

APPENDIX C. CURRENT RELATIONS IN AN OSCILLATING CIRCUIT WITH A CLOSED SECONDARY

The combination of two magnetically coupled circuits, one containing resistance, inductance, and capacitance in series while the other contains only resistance and inductance (as shown in fig. 14), is often met with in the theory of ignition apparatus and induction coils. Iolo Jones[5] has discussed in some detail the frequencies and damping of the oscillations which may occur in such a system and has worked out numerical values for particular cases.

[5] Phil. Mag. ser. 6, **39**, p. 553; 1920.

In the following paragraphs a somewhat more general treatment will be given, together with expressions for the constants of integration pertaining to any given initial conditions.

These relations can be applied to a number of the processes occurring in the operation of ignition apparatus. Among these are: (1) the building up of voltage in the "closed-coil" model in which the eddy currents in the core are assumed to flow in a fixed tertiary circuit coupled magnetically to the simple "single-coil model," (2) the building up of voltage when the coil is working with a low-resistance carbon deposit across its secondary terminals, and (3) the transfer of energy from primary to secondary immediately after the secondary spark gap has become conducting.

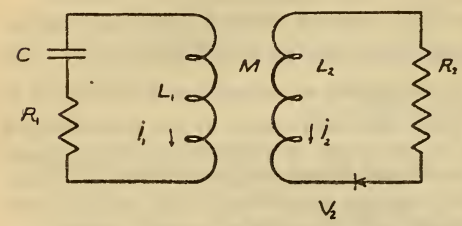

FIG. 14.—*Oscillatory circuit coupled to a closed secondary circuit*

(*a*) GENERAL EQUATIONS

The basic equations for the circuits shown in Figure 14 are

$$L_1\frac{di_1}{dt}+R_1i_1+M\frac{di_2}{dt}+v_1=0 \tag{1c}$$

and

$$L_2\frac{di_2}{dt}+R_2i_2+M\frac{di_1}{dt}+V_2=0 \tag{2c}$$

which express the fact that the sum of all the voltages in each circuit is zero. Here v_1 is the instantaneous value of the voltage across the condenser terminals, and the constant voltage V_2 is introduced to represent an emf of rotation or the effect of the voltage drop (experimentally found to be nearly constant) across the arc at the spark gap in the application (3) listed above. In the other applications V_2 will be set equal to zero.

Equations (1c) and (2c) combined with the relation

$$i_1=C_1\frac{dv_1}{dt} \tag{3c}$$

between the instantaneous values i_1 and v_1 of primary current and of the voltage across the primary condenser, respectively, serve to give the differential equations for the three variables i_1, i_2, and v_1 separately. These are

$$L_1L_2(1-k^2)\frac{d^3i_1}{dt^3}+(R_1L_2+R_2L_1)\frac{d^2i_1}{dt^2}+\left(R_1R_2+\frac{L_2}{C_1}\right)\frac{di_1}{dt}+\frac{R_2}{C_1}i_1=0 \tag{4c}$$

$$L_1L_2(1-k^2)\frac{d^3v_1}{dt^3}+(R_1L_2+R_2L_1)\frac{d^2v_1}{dt^2}+\left(R_1R_2+\frac{L_2}{C_1}\right)\frac{dv_1}{dt}+\frac{R_2}{C_1}v_1=0 \tag{5c}$$

and

$$L_1L_2(1-k^2)\frac{d^3i_2}{dt^3}+(R_1L_2+R_2L_1)\frac{d^2i_2}{dt^2}+\left(R_1R_2+\frac{L_2}{C_1}\right)\frac{di_2}{dt}+\frac{R_2}{C_1}i_2+\frac{V_2}{C_1}=0 \tag{6c}$$

These equations are all of the same form except that (6c) has the constant term $\frac{V_2}{C_1}$ which leads to a corresponding particular integral $i_2=-\frac{V_2}{R_2}$ in the solution of (6c); while the solutions of (4c) and (5c) consist of the complementary function only. This complementary function has the form

$$A'e^{m_1t}+B'e^{m_2t}+C'e^{m_3t} \tag{7c}$$

or

$$Ae^{\alpha t}\cos\beta t+Be^{\alpha t}\sin\beta t+Ce^{m_1t} \tag{8c}$$

where m_1, m_2, and m_3 are the roots of the auxiliary equation

$$L_1L_2(1-k^2)m^3+(R_2L_1+R_1L_2)m^2+\left(R_1R_2+\frac{L_2}{C_1}\right)m+\frac{R_2}{C_1}=0 \tag{9c}$$

Form (7c) applies if all three roots of equation (9c) are real, and form (8c) applies if one root is real and the other two are conjugate complex quantities, so that

$$m_2=\alpha+j\beta,\ m_3=\alpha-j\beta \tag{10c}$$

where α and β are real.

The system shown in Figure 14 may be described by an alternative set of constants defined as follows:

ERRATA

In Scientific Paper No. 543, vol. 21, p. 681, the two lines following equation (13c) should read:

and the roots q_1, q_2, q_3 or q_1, $\delta+j\gamma$, $\delta-j\gamma$ are equal to the corresponding roots of (12c) or of (9c) each multiplied by T (e. g., $q_1=m_1\ T$, $\gamma=\beta T$, etc.).

Please make the above corrections by pen in Scientific Paper No. 543 or paste this Errata sheet between pages 680 and 681.

66452—27

and the roots q_1, q_2, q_3 or q_1, $\delta+j\gamma$, $\delta-j\gamma$ are equal to the corresponding roots of (12c) or of (9c) each divided by T (e.g. $q_1=\frac{m_1}{T}$, $\gamma=\frac{\beta}{T}$, etc.)

For the values of k, r, and s physically possible the coefficients of equation (13c) are all positive and it can have no positive roots. Hence, q_1 must be negative and real. In the general case the condition that all three roots be real is that

$$4\ (b^2-c)^3\leqq(2b^3+d-3\ bc)^2 \tag{14c}$$

where

$$b=\frac{r+s}{3(1-k^2)},\quad c=\frac{rs+1}{3(1-k^2)},\quad d=\frac{s}{1-k^2} \tag{15c}$$

If $r=0$ this condition is equivalent to

$$(1-k^2)\leqq\frac{9\ s^2-2\pm2\sqrt{(1-3s^2)^3}}{27\ s^2} \tag{16c}$$

and the region of real roots lies in the range where

$$s < \frac{1}{3} \text{ and } k^2 > \frac{8}{9}$$

In Figure 15 are plotted on the k^2—s plane the boundaries between the regions of real and complex roots for several values of r. For small values of s an approximate criterion for real roots is

$$(1-k^2) \leqq \frac{(r+sk^2)^2}{4} \tag{17c}$$

and the dotted curves in Figure 15 show the trend of values obtained from this equation (17c). It will be seen from Figure 16 that the nonoscillating

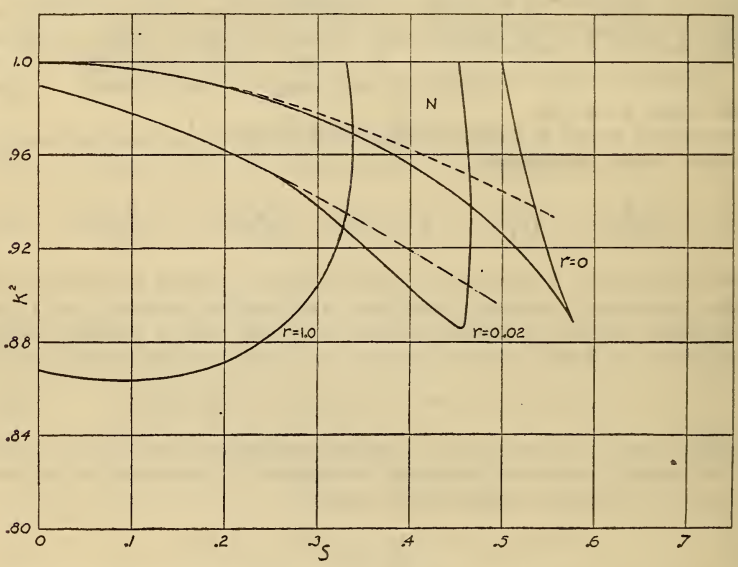

FIG. 15.—*Part of the k^2-s plane showing for three different values of r the region within which the phenomena are nonoscillatory*

Dotted lines show boundary as located by the approximate equation 4 $(1-k^2)=(r+sk^2)^2$

region "N" occupies only a very small part of the region in the k^2—s plane in which the system may be operating.

The solution of equation (13c) in the general case for given values of k^2, r, and s is very laborious but has been carried through by Iolo Jones.[6] Corresponding results of sufficient accuracy for many purposes can be obtained by solving equation (13c) for s and obtaining

$$s = -\frac{q\{1+r+q^2(1-k^2)\}}{1+rq+q^2} \tag{18c}$$

The desired values of r and k and a series of arbitrary real, negative values of q may then be inserted in (18c) and the corresponding value of s for each

[6] Loc. cit.

q computed. The original equation can then be depressed and q_2 and q_3 corresponding to each q_1 and s found. A graph of these values as ordinates against s as abscissa can then be used to give the roots for other given values of s.

When s has thus been determined for an assumed q_1, the other roots may be found at once by the equations

$$\delta = -\left(\frac{q_1}{2} + \frac{r+s}{2(1-k^2)}\right) \tag{19c}$$

$$\gamma = \sqrt{\frac{q_1^3(1-k^2)^2 + 2q_1^2(1-k^2)\,(s+r) + q_1(r+s)^2 + 4s(1-k^2)}{-4q_1(1-k^2)^2}} \tag{20c}$$

For very large or very small values of s equation (13c) can be factored and approximate values for q_1 found directly.

Table 1 gives in compact form the equations resulting in the several cases. In most practical cases r is small, so that the simplified formulas obtained by

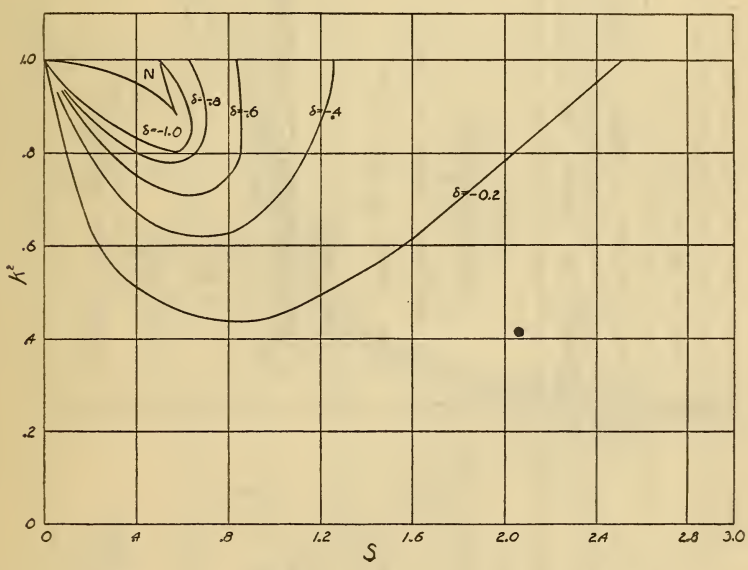

FIG. 16.—*Map of the k^2-s plane showing at N the region within which the phenomena are nonoscillatory for $r=o$*

The outer contour lines correspond to the successive values of δ marked on them

setting $r=0$ are applicable. Numerical values for γ and q_1 have been worked out for this case and are plotted as ordinate in Figures 17 and 18 against s as abscissa for several values of k^2. Figure 16 gives the values for δ corresponding to various possible combinations of k^2 and s by indicating the contours along which δ has assigned constant values.

In the most general case the primary and secondary currents and the condenser voltage may have any initial values I_1, I_2, and V_1, respectively at the instant $t=0$. The constants of integration A, B, and C (or A', B', C') in equations (7c) and (8c) are linear functions of these three initial values and of

TABLE 1.—*Formulas for roots of cubic equation (13c)*

$(1-k^2)q^3+(s+r)q^2+(1+rs)q+s=0$				
Conditions for oscillations	$r=r$	$4(b^2-c)^3 \geq (2b^3+d-3bc)^2$ where $b=\frac{r+s}{3(1-k^2)}$, $c=\frac{1+rs}{3(1-k^2)}$, $d=\frac{s}{1-k^2}$		
	$r=0$	$(1-k^2)=\frac{9s^2-2\pm 2\sqrt{(1-3s^2)^3}}{27s^2}$ all roots can be real only when $s<\frac{1}{\sqrt{3}}$ and $k^2>\frac{8}{9}$		
Values of roots for oscillatory case	$r=r$	$s=$ small $(q+s)\{(1-k^2)q^2+(r+sk^2)q+1\}=0$ $q_1=-s$ $q_2=\delta+j\gamma$, $q_3=\delta-j\gamma$ $\delta=\frac{-(r+sk^2)}{2(1-k^2)}$ $\gamma=\sqrt{\frac{1}{1-k^2}-\frac{(r+sk^2)^2}{4(1-k^2)^2}}$ $\gamma^2+\delta^2=\frac{1}{1-k^2}$	General case $s=\frac{-q\{1+r+(1-k^2)q^2\}}{1+rq+q^2}$ for arbitrary values of $q=q_1$ find s, then $q_2, q_3=\delta\pm j\gamma$ $\delta=-\left\{\frac{q_1}{2}+\frac{s+r}{2(1-k^2)}\right\}$ $\gamma=\sqrt{\frac{q_1^3(1-k^2)^2+2q_1^2(1-k^2)(s+r)+(s+r)^2q_1+4s(1-k^2)}{-4q_1(1-k^2)^2}}$ $\gamma^2+\delta^2=-\frac{s}{q_1(1-k^2)}$	$s=$ large $(q+\frac{s}{1-k^2})\{q^2+(r+\frac{k^2}{s})q+1\}=0$ $q_1=-\frac{s}{1-k^2}$ $q_2=\delta+j\gamma$, $q_3=\delta-j\gamma$ $\delta=-\frac{1}{2}(r+\frac{k^2}{s})$ $\gamma=\sqrt{1-\frac{(r-\frac{k^2}{s})^2}{4}}$ $\gamma^2+\delta^2=1$
	$r=0$	$\delta=\frac{-sk^2}{2(1-k^2)}$ $\gamma=\sqrt{\frac{1}{1-k^2}-\frac{q^2k^2(1-\frac{3}{2}k^2)}{(1-k^2)^2}}$	$\delta=-\left\{\frac{q_1}{2}+\frac{s}{2(1-k^2)}\right\}$ $\gamma=\frac{s}{2(1-k^2)}\sqrt{-\left\{1+\frac{q_1}{s}(1-k^2)\right\}^2-\frac{4(1-k^2)}{q_1 s}}$	$\delta=-\frac{k^2}{2s}$ $\gamma=\sqrt{1-\frac{k^4}{4s^2}}$

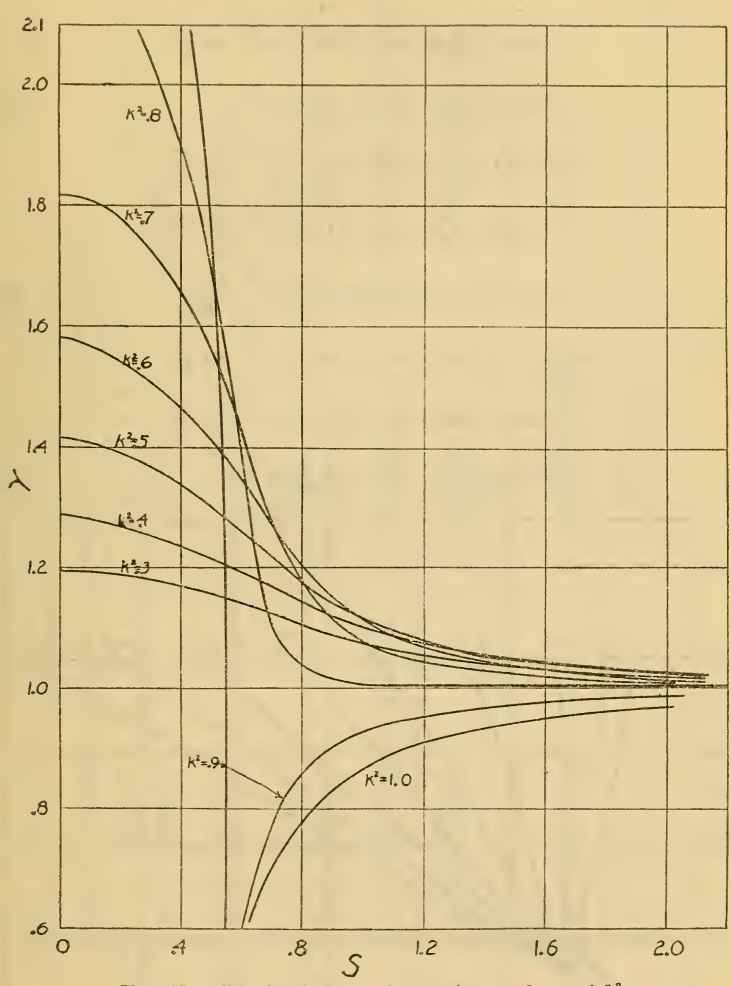

FIG. 17.—*Graph of γ v. s for various values of k^2*

V_2. The coefficients of these values can conveniently be represented by the notation indicated in the following equations:

$$i_1=(A_{11}I_1+A_{12}I_2+F_{11}V_1+F_{12}V_2)\,e^{\frac{\delta t}{T}}\cos\frac{\gamma t}{T}$$
$$+(B_{11}I_1+B_{12}I_2+G_{11}V_1+G_{12}V_2)\,e^{\frac{\delta t}{T}}\sin\frac{\gamma t}{T}$$
$$+(C_{11}I_1+C_{12}I_2+H_{11}V_1+H_{12}V_2)\,e^{\frac{q_1 t}{T}} \tag{21c}$$

$$i_2=(A_{21}I_1+A_{22}I_2+F_{21}V_1+F_{22}V_2)\,e^{\frac{\delta t}{T}}\cos\frac{\gamma t}{T}$$
$$+(B_{21}I_1+B_{22}I_2+G_{21}V_1+G_{22}V_2)\,e^{\frac{\delta t}{T}}\sin\frac{\gamma t}{T}$$
$$+(C_{21}I_1+C_{22}I_2+H_{21}V_1+H_{22}V_2)\,e^{\frac{q_1 t}{T}}-\frac{V_2}{R_2} \tag{22c}$$

$$v_1=(A_{v1}I_1+A_{v2}I_2+F_{v1}V_1+F_{v2}V_2)\,e^{\frac{\delta t}{T}}\cos\frac{\gamma t}{T}$$
$$+(B_{v1}I_1+B_{v2}I_2+G_{v1}V_1+G_{v2}V_2)\,e^{\frac{\delta t}{T}}\sin\frac{\gamma t}{T}$$
$$+(C_{v1}I_1+C_{v2}I_2+H_{v1}V_1+H_{v2}V_2)\,e^{\frac{q_1 t}{T}} \tag{23c}$$

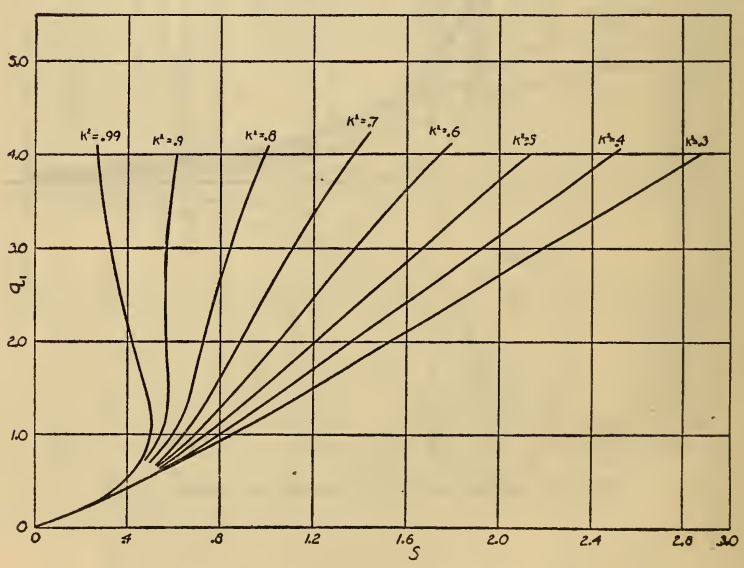

FIG. 18.—*Graph of q_1 v. s for various values of k^2*

The exact values of the individual coefficients in terms of γ, δ, q, k^2, r, and s are given in Table 2.

The corresponding coefficients of I_1 for the case of damped impulses are given in equation (64) of Bureau of Standards Scientific Paper No. 424, p. 442.

Table 2.—*Coefficients of terms in equations (21 c), (22 c), and (23 c)*

	Coefficients of I_1	Coefficients of I_2	Coefficients of V_1	Coefficients of V_2
Coefficients for i_1	$A_{11}=\frac{(1-k^2)(\gamma^2+\delta^2+g_1^2)+\lambda g_1}{(1-k^2)\{\gamma^2+(\delta-g_1)^2\}}$	$A_{12}=\frac{-kn\Delta g_1}{(1-k^2)\{\gamma^2+(\delta-g_1)^2\}}$	$F_{11}=\frac{+c(g_1+\Delta)}{T(1-k^2)\{\gamma^2+(\delta-g_1)^2\}}$	$F_{12}=\frac{-c_1kg_1}{Tm(1-k^2)\{\gamma^2+(\delta-g_1)^2\}}$
	$B_{11}=\frac{-\delta(1-k^2)(\gamma^2+\delta^2-g_1^2)-\lambda(\gamma^2+\delta^2-\delta g_1)}{\gamma(1-k^2)\{\gamma^2+(\delta-g_1)^2\}}$	$B_{12}=\frac{kn\Delta(\gamma^2+\delta^2-\delta g_1)}{\gamma(1-k^2)\{\gamma^2+(\delta-g_1)^2\}}$	$G_{11}=\frac{-c_1[\gamma^2+\delta^2-\delta g_1+\Delta(\delta-g_1)]}{T\gamma(1-k^2)\{\gamma^2+(\delta-g_1)^2\}}$	$G_{12}=\frac{c_1k\{\gamma^2+\delta^2-\delta g_1\}}{Tm\gamma(1-k^2)\{\gamma^2+(\delta-g_1)^2\}}$
	$C_{11}=\frac{-g_1(\gamma^2+\delta^2-1)}{\gamma^2+(\delta-g_1)^2}$	$C_{12}=\frac{+kn\Delta g_1}{(1-k^2)\{\gamma^2+(\delta-g_1)^2\}}=-A_{12}$	$H_{11}=\frac{-c(g_1+\Delta)}{T(1-k^2)\{\gamma^2+(\delta-g_1)^2\}}=-F_{11}$	$H_{12}=\frac{c_1kg_1}{Tm(1-k^2)\{\gamma^2+(\delta-g_1)^2\}}=-F_{12}$
Coefficients for i_2	$A_{21}=\frac{-k(1+\lambda g_1)}{n(1-k^2)\{\gamma^2+(\delta-g_1)^2\}}$	$A_{22}=\frac{g_1(1-k^2)(g_1-2\delta)+\Delta(g_1+\lambda)}{(1-k^2)\{\gamma^2+(\delta-g_1)^2\}}$	$F_{21}=\frac{-c_1kg_1}{Tm(1-k^2)\{\gamma^2+(\delta-g_1)^2\}}$	$F_{22}=\frac{g_1(1-k^2)(g_1-2\delta)+\Delta(g_1+\lambda)}{R_2(1-k^2)\{\gamma^2+(\delta-g_1)^2\}}=\frac{A_{22}}{R_2}$
	$B_{21}=\frac{k[\delta-g_1+\lambda(\gamma^2+\delta^2-\delta g_1)]}{m\gamma(1-k^2)\{\gamma^2+(\delta-g_1)^2\}}$	$B_{22}=\frac{-g_1(1-k^2)(\gamma^2-\delta^2+\delta g_1)-\Delta(\gamma^2+\delta^2-\delta g_1)-\lambda\Delta(\delta-g_1)}{\gamma(1-k^2)\{\gamma^2+(\delta-g_1)^2\}}$	$G_{21}=\frac{c_1k(\gamma^2+\delta^2-\delta g_1)}{Tm\gamma(1-k^2)\{\gamma^2+(\delta-g_1)^2\}}$	$G_{22}=\frac{-g_1(1-k^2)(\gamma^2-\delta^2+\delta g_1)-\Delta(\gamma^2+\delta^2-\delta g_1)-\lambda\Delta(\delta-g_1)}{R_2\gamma(1-k^2)\{\gamma^2+(\delta-g_1)^2\}}=\frac{B_{22}}{R_2}$
	$C_{21}=\frac{+k(1+\lambda g_1)}{m(1-k^2)\{\gamma^2+(\delta-g_1)^2\}}=-A_{21}$	$C_{22}=\frac{(1-k^2)(\gamma^2+\delta^2)-\Delta(g_1+\lambda)}{(1-k^2)\{\gamma^2+(\delta-g_1)^2\}}$	$H_{21}=\frac{+c_1kg_1}{Tm(1-k^2)\{\gamma^2+(\delta-g_1)^2\}}=-F_{21}$	$H_{22}=\frac{(1-k^2)(\gamma^2+\delta^2)-\Delta(g_1+\lambda)}{R_2(1-k^2)\{\gamma^2+(\delta-g_1)^2\}}=\frac{C_{22}}{R_2}$
Coefficients for v_1	$A_{V1}=\frac{Tg_1(\gamma^2+\delta^2-1)}{c_1\{\gamma^2+(\delta-g_1)^2\}}$	$A_{V2}=\frac{-Tkn\Delta}{c_1(1-k^2)\{\gamma^2+(\delta-g_1)^2\}}$	$F_{V1}=1+\frac{g_1+\Delta}{g_1(1-k^2)\{\gamma^2+(\delta-g_1)^2\}}$	$F_{V2}=\frac{-k}{m(1-k^2)\{\gamma^2+(\delta-g_1)^2\}}$
	$B_{V1}=\frac{T[(1-k^2)(\gamma^2-\delta^2+g_1^2)-\lambda(\delta-g_1)]}{c_1\gamma(1-k^2)\{\gamma^2+(\delta-g_1)^2\}}$	$B_{V2}=\frac{Tkn\Delta(\delta-g_1)}{c_1\gamma(1-k^2)\{\gamma^2+(\delta-g_1)^2\}}$	$G_{V1}=\frac{\Delta(\gamma^2-\delta^2+\delta g_1)-(\gamma^2+\delta^2)(\delta-g_1)}{\gamma(1-k^2)(\gamma^2+\delta^2)\{\gamma^2+(\delta-g_1)^2\}}$	$G_{V2}=\frac{k(\delta-g_1)}{m\gamma(1-k^2)\{\gamma^2+(\delta-g_1)^2\}}$
	$C_{V1}=\frac{-Tg_1(\gamma^2+\delta^2-1)}{c_1\{\gamma^2+(\delta-g_1)^2\}}=-A_{V1}$	$C_{V2}=\frac{+Tkn\Delta}{c_1(1-k^2)\{\gamma^2+(\delta-g_1)^2\}}=-A_{V2}$	$H_{V1}=\frac{-(g_1+\Delta)}{g_1(1-k^2)\{\gamma^2+(\delta-g_1)^2\}}=1-F_{V1}$	$H_{V2}=\frac{+k}{m(1-k^2)\{\gamma^2+(\delta-g_1)^2\}}=-F_{V2}$

(b) APPLICATION TO EFFECT OF EDDY CURRENTS

The first important application of these equations is to the building up of voltage after the instant of "break" in the case when the actual secondary circuit is open and the eddy currents in the core are simulated by a closed tertiary circuit. In this case the primary circuit of the closed-coil model here treated may be taken as having the same self-inductance as one (say, the primary) circuit of the actual magneto. The condenser C_1 should then be taken as having the total effective capacitance of the windings referred to the same side. This value, referred to the primary, is given by the sum of the actual primary capacitance and n^2 times the effective secondary capacitance. The best estimate of the value to be assigned to R_1 is obtained by the equation

$$R_1' = \left(\frac{C_1}{C_1+n^2C_2}\right)^2 R_1 + \left(\frac{n^2C_2}{C_1+n^2C_2}\right)^2 R_2 \tag{24c}$$

where R_1 and R_2 are the actual resistances of the primary and secondary windings. In most practical cases, however, the resulting value of r will be found to be negligibly small in comparison with unity.

The constants L_2, R_2, and M of the model should be such as to give the same reaction upon the main windings as do the actual eddy currents in the core and pole pieces, but since we are interested only in these reactions and not in the actual magnitude of the eddy currents themselves we may arbitrarily take $n=1$ and consider the secondary circuit completely defined by its coupling k_e and either its own time constant T_e or the corresponding ratio $s_e=\frac{T}{T_e}=R_e\sqrt{\frac{C_1}{L_1}}$.

As is indicated in Appendix D, there is great difficulty in experimentally obtaining values for k_e and T_e because of the fact that the eddy-current circuit shows a marked "skin effect" so that the "constants" of the circuit in which they may be considered as flowing depend upon both the rapidity with which the flux changes occur and with the magnetic permeability (and hence with the flux density). It is easily possible by bridge measurements with alternating current of any desired frequency to determine the values of k_e and T_e for a circuit which would have at that frequency and flux density the same reaction on the windings as does the group of eddy-current circuits actually present. However, it is not feasible to make such measurements with the value of flux density occurring in the actual operation of the coil because of the excessive heating which would be produced. Observed values of k_e and T_e, therefore, must be extrapolated considerably in the direction of larger k_e and smaller T_e if they are to approximate the normal operating values of these constants. Values observed at 3,000 cycles have shown k_e^2 ranging from 0.91 to 0.40 and T_e ranging from 0.23×10^{-4} to 2.4×10^{-4}, in the case of 10 typical ignition systems. The corresponding range of s_e was from 0.5 to 2 and r did not exceed 0.01.

The effect of any given values of k_e and T_e on the voltage induced at the condenser terminals can be found directly from equation (23c) and numerical computations have been carried through with slide-rule accuracy for the case where $r=0$ for a considerable range of s. The crest value of v_1 has been estimated by combining the three main terms of equation (23c) for several values of t near that giving the crest voltage. The final results are plotted in Figure 19, the crest voltages being expressed as fractions of $I_1\sqrt{\frac{L_1}{C_0}}$.

To represent on the $N\phi$–I diagram the state of affairs assumed in this closed-coil model we must note that i_1 in the model is equivalent to i_1+ni_2 on

the diagram, since it represents the effect of all the currents in both of the actual windings, while i_2 of the model corresponds to i_e of the diagram. We may, therefore, fix the locus $F\ L'\ L\ G$ of Figure 4 or Figure 6 by plotting simultaneous values of $N\phi_1$ and i_1. Since at $t=0$ $I_2=0$ $V=0$ and also $V_2=0$ we are concerned only with the coefficients of I_1 and

$$N_1\phi_1=L_1\ [(A_{11}+knA_{21})\ e^{\alpha t}\cos\beta t+(B_{11}+knB_{21})\ e^{\alpha t}\sin\beta t+(C_{11}+knC_{21})\ e^{m_1 t}]\ I_1 \tag{25c}$$

while

$$i_1=(A_{11}\,e^{\alpha t}\cos\beta t+B_{11}\,e^{\alpha t}\sin\beta t+C_{11}\,e^{m_1 t})\ I_1$$

and (26c)

$$i_2=(A_{21}\,e^{\alpha t}\cos\beta t+B_{21}\,e^{\alpha t}\sin\beta t+C_{21}\,e^{m_1 t})\ I_1$$

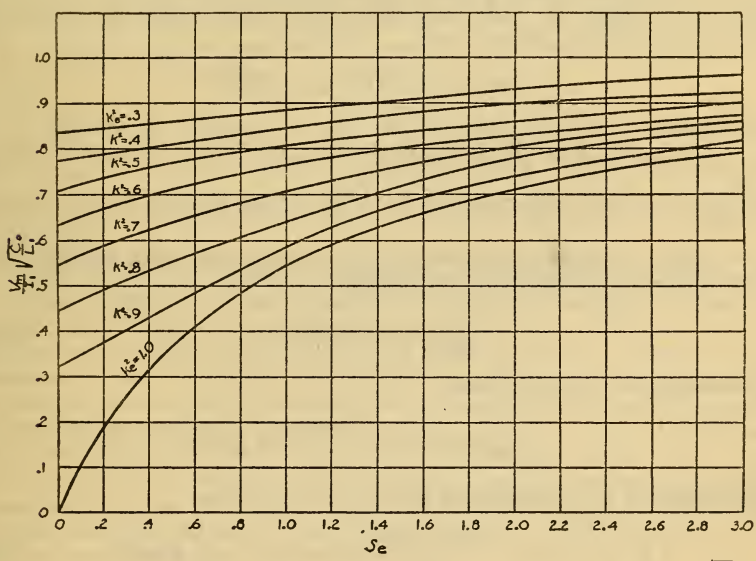

FIG. 19.—*Graph of crest value of v_1, expressed as a fraction of $I_1\sqrt{\frac{L_1}{C_0}}$, plotted against s_e for various values of k_e^2*

For use when the secondary terminals are insulated but eddy currents are present

For many purposes an exact fixing of the locus $F\ L'\ L\ G$ is not required and an approximate procedure can be developed from the following considerations. If s_e is very small we find from Table 2 that

$$N_1\phi_1=(1-k_e^2)L_1I_1e^{\alpha t}\cos\beta t+L_1I_1k_e^2e^{m_1 t} \tag{27c}$$

and

$$i_1=I_1e^{\alpha t}\cos\beta t \tag{28c}$$

Hence

$$N_1\phi_1=(1-k_e^2)L_1i_1+k_e^2L_1I_1e^{m_1 t} \tag{30c}$$

and also m_1 is very small so that the last term is practically constant. On this basis the locus $F\ L'\ L\ G$ is a straight line passing through F and having a slope $(1-k_e^2)\ L_1$. Point G is located at $N_1\ \phi_1=k_e^2\ L_1\ I_1$ and hence divides $P\ E$ into segments having the ratio $E\ G:G\ P=1-k_e^2:k_e^2$.

If $s_e=\infty$ which is equivalent to assuming the eddy currents to be absent, the locus coincides with $F\ M'\ M\ P$ for all values of k_e and is also a straight

line. For intermediate values of s_e the locus has an intermediate position, but is still very nearly a straight line as is shown by the curve $F\ L\ G$ in Figure 6, which has been plotted from values computed for the case $s_e=0.38$, $k_e=0.5$, $r=0.0015$.

If the line were exactly straight, the point G could be located by the relation that ratio of $E\ G$ to $E\ P$ is equal to the square of the ratio of the actual crest voltage to the value for $s=\infty$. On this assumption the family of curves on the left side of Figure 6 have been computed. To locate point G corresponding to given values of k_e and s_e, it is necessary merely to follow the course indicated by the dotted line. A straight line connecting G and F then gives the locus.

By the definition of the locus $F\ G$ in Figure 6 the distance $N\ L$ is proportional to the magnetomotive forces of the currents in the coils, but the flux turns $P\ N$ require for their maintenance the magnetomotive force resulting from a current $N\ M$. Hence, since

$$N_1\ \phi_1=L_1\ i_1+M_e\ i_e=L_1\ (i_1+k_e\ i_e) \tag{31c}$$

the distance $L\ M$ must equal (to the scale of currents) the quantity $k_e\ I_e$. An additional locus $F\ B$ can, therefore, be drawn so that $L\ B=\frac{LM}{k_e}$ and the distance $L\ B$ will then represent the eddy current directly, on the basis of $L_e=L_1$.

To study the energy relations involved we may start with equation (2c) above and set $V_2=0$ and $L_2=L_e=L_1$ getting

$$L_1\frac{d}{dt}(i_e+k_e i_1)+R_e i_e=0 \tag{32c}$$

Combining this with (31c) gives

$$k_e\frac{d}{dt}N_1\phi_1+L_1(1-k_e^2)\frac{di_e}{dt}+R_e i_e=0$$

Multiplying by i_e and integrating from $t=t_1$ to $t=t_2$ gives

$$\int_1^2 k_e i_e d(N_1\phi_1)=-\frac{L_1(1-k_e^2)}{2}\{(I_e)^2{}_2-(I_e)^2{}_1\}-\int_1^2 R_e i_e^2 dt \tag{33c}$$

If this change is, for example, in Figure 6 that from point N' to point N the left-hand member is equal to the area $L'\ M'\ M\ L$. The last term on the right of equation (33c) is equal to the energy dissipated in joule heating during the time interval t_2-t_1. The first term on the right side of equation (33c) is the energy rendered permanently unavailable by the growth of the eddy currents between t_1 and t_2.

This last relation may be seen by considering that the most efficient possible utilization of the magnetic energy stored at the time t_2 would be obtained by closing the primary circuit by a conducting path (or spark) of zero resistance. If this is done, the state point will move from L to M without any further change in the linkages and the current in the coil will then be at time t_3

$$(I_1)_3=(I_1)_2+k_e(I_e)_2 \tag{34c}$$

and the energy W_3 then stored in the field is

$$W_3=\frac{L}{2}(I_1)^2{}_3=\frac{L}{2}(I_1)^2{}_2+k_e L(I_1)_2(I_e)_2+\frac{k_e^2 L}{2}(I_e)^2{}_2 \tag{35c}$$

The total stored energy W_2 under condition 2 was

$$W_2=\frac{L}{2}(I_1)^2{}_2+M(I_1)_2(I_e)_2+\frac{L}{2}(I_e)^2{}_2 \tag{36c}$$

and the difference

$$W_2-W_3=\frac{(1-k_e^2)L}{2}(I_e)^2{}_2 \tag{37c}$$

shows the net loss to the primary circuit caused by the existence of $(I_e)_2$. This result is the same as the first term on the right side of equation (33c).

The preceding discussion has not taken account of any electromotive forces resulting from the rotation of the magneto armature. These electromotive forces are usually negligible, but when the machine is operating at high speeds and full advance they may become appreciable in comparison with the voltage induced by induction-coil action. If E_1 is the electromotive force of rotation generated in the winding and E_2 that in the eddy-current circuit, the foregoing equations may still be applied by considering that in equations (1c) and (2c) v_1 represents the combination

$$v_1=v_1'-E_1 \tag{38c}$$

where now v_1' is the voltage across the condenser terminals, and

$$V_2=-E_2 \tag{39c}$$

E_1 and E_2 can reasonably be assumed to be constant during the short interval of period 2.

(c) APPLICATION TO EFFECT OF SHUNTING CONDUCTANCE ON SECONDARY

Another application of these equations is to the building up of voltage in cases where the secondary terminals of the magneto or induction coil are shunted by a conducting path (such as a layer of carbon) of relatively low resistance S. If we consider the classical two-coil model of the apparatus, we see that the secondary condenser is directly shunted by the conducting path S, and that the currents in the condenser and in S reach a mutual equilibrium at a much faster rate, unless S is very large, than do other parts of the circuit. We may, therefore, assume that the voltage across the condenser is at all times i_2S and that the current through the condenser is so small in comparison with that through S that we may neglect it. We thus arrive at a pair of circuits similar to those of Figure 14.

In this case we should use for C_1 the capacitance of the primary condenser itself and for L_1 the primary inductance. k is now the coupling between the real primary and secondary coils and is very nearly unity. The secondary resistance R_2 may usually be neglected, but if appreciable it may be added to S to give the value to be assigned to R_2 in the model and the terminal voltage may then be taken as the factor $\frac{S}{R_2+S}$ of the computed value.

The range of k^2 is in most cases from 0.88 to 0.98 and the range of S which, is of most interest in ignition work, is over those values which will reduce the crest voltage into the range of the sparking voltages of spark plugs. In a group of 10 ignition systems examined the values of S, which reduced the crest voltage to 5,000 volts, ranged from 30,000 to 200,000 ohms, and the corresponding values of s ranged from 0.03 to 0.125. When the resistance shunting the secondary was greater than such as to make $s=0.125$, the crest voltage exceeded 5,000 volts. In these systems r was less than 0.03 in all cases. Hence, in this case also the phenomena are oscillatory, but the values of γ are much higher than in the preceding applications. The voltage at the spark plug terminals is in this case not v_1 but i_2S, and hence Figure 19 is not applicable.

The secondary crest voltage is given as a function of time by

$$i_2S=I_1S\left(A_{21}e^{\frac{\delta t}{T}}\cos\frac{\beta t}{T}+B_{21}e^{\frac{\delta t}{T}}\sin\frac{\beta t}{T}+C_{21}e^{\frac{q_1 t}{T}}\right) \tag{40c}$$

which on inserting the values for the coefficients, becomes for $r=0$

$$i_2S=nI_1\sqrt{\frac{L_1}{C_1}}\frac{sk}{(1-k^2)(\gamma^2+(\delta-q_1)^2)}\left[e^{\frac{q_1 t}{T}}+e^{\frac{\delta t}{T}}\left\{\left(\frac{(\delta-q_1)}{\gamma}\right)\sin\frac{\gamma t}{T}-\cos\frac{\gamma t}{T}\right\}\right] \tag{41c}$$

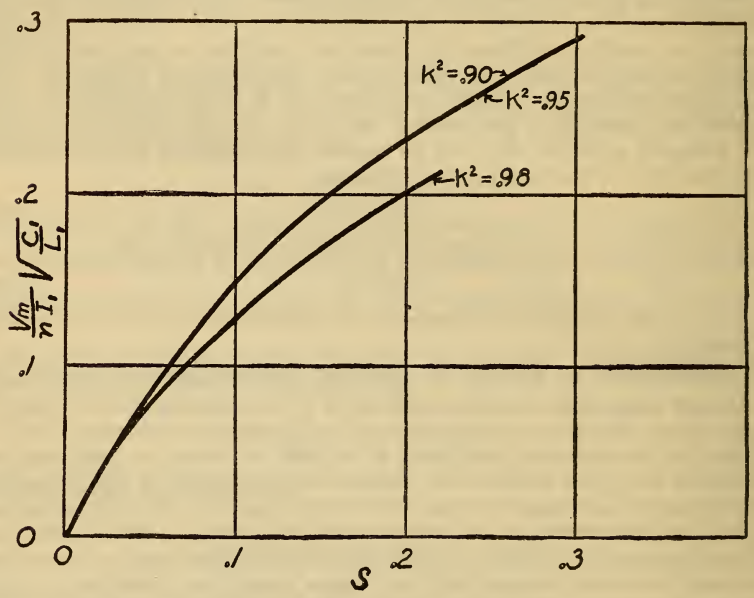

FIG. 20.—*Graph of secondary crest voltage* (i_2S) *expressed as a fraction of* $I_1n\sqrt{\frac{L_1}{C_1}}$

For use in cases where the secondary is shunted by resistance.

By computing values of i_2S for several values of t and plotting the results the crest value of the voltage can be determined. This has been done for $k^2=0.90$, 0.95, 0.98 for several values of s, and the crest voltages thus computed, expressed in terms of $nI_1\sqrt{\frac{L_1}{C_1}}$, are plotted against s in Figure 20. It will be noted from equation (41c) that as s approaches zero, while $1-k^2$ remains finite and $r=0$, i_2S approaches $2\,kns\,I_1\sqrt{\frac{L_1}{C_1}}$. Figure 20 shows that for values of k^2 between 0.90 and 0.95 the crest voltage is so nearly independent of k^2 that the curves for different values of k^2 practically coincide.

(*d*) APPLICATION TO TRANSFER OF ENERGY FROM PRIMARY TO SECONDARY

A third application of the foregoing equations is to period 3, which covers the transition from the conditions at the end of period 2 to the beginning of period 4. Under normal conditions at the beginning of period 3 the voltage across the primary condenser is equal to $V_1=\frac{V_g}{n}$, where V_g is the breakdown

voltage of the spark gap, the currents flowing in the primary and secondary circuits and charging their respective capacitances may be denoted by I_1 and I_2, and are materially less than the values I_b and I_b/n, respectively. There are also eddy currents present in the metallic masses in and near the core which have an appreciable magnetizing effect. At the end of the transition the primary voltage and current have sunk to negligibly small values. The secondary voltage is substantially constant at a value V_s, which is that required to sustain the arc across the spark plug gap, and which is fairly constant during period 4. The secondary current has a considerable magnitude, but decreases at a slow, steady rate, and the eddy currents have considerably decreased.

Here, again, a complete mathematical handling of the phenomena becomes impracticable, but a suggestion of the true state of affairs may, perhaps, be obtained by considering two parts of the process as occurring independently. We will, therefore, first neglect the eddy current and study the energy transfers between primary and secondary and later neglect the primary circuit and study the energy transfer between eddy circuit and secondary.

For the former case we again have the circuits effectively as in Figure 14. The condenser-circuit constants are identically those of the actual primary circuit and the secondary circuit has the same self and mutual inductance as the actual winding. The secondary capacitance can be neglected for the same reasons as in the preceding case. The resistance of the secondary circuit consists of the resistance of the winding (2,000 to 6,000 ohms) plus that of the spark gap. The latter is very difficult to estimate. In radiotelegraphic spark transmitting sets the resistance of the gap is usually considered to be only a few ohms at most but may well be somewhat greater in the present case because of the small current flowing.

From this it appears that while the value of k^2 in this case is identical with that to be used in computing the effect of a shunting resistance during period 2, the value of s, which is proportional to the resistance of the secondary circuit, is materially smaller. In Figures 15 and 16, therefore, we are interested in a region between $k^2=0.90$ and 0.98 and between $s=0$ and $s=0.05$, and hence in an oscillatory phenomenon. Since at best only a rough approximation can be obtained, it will suffice to use for the several coefficients the values which they approach for small values of s. On this basis we have

$$i_1=\left[+I_1+kns^2I_2-s^3k^3\sqrt{\frac{C}{L}}V_1+\frac{ks}{n}\sqrt{\frac{C}{L}}V_s\right]e^{\frac{\delta t}{T}}\cos\frac{\gamma t}{T}$$
$$+\left[+\frac{sk^2}{2\sqrt{1-k^2}}I_1+\frac{kns}{\sqrt{1-k^2}}I_2-\sqrt{\frac{C}{L(1-k^2)}}V_1+\frac{k}{n}\sqrt{\frac{C}{L(1-k^2)}}Vs\right]e^{\frac{\delta t}{T}}\sin\frac{\gamma t}{T}$$
$$+\left[-s^2k^2I_1+kns^2I_2+s^3k^3\sqrt{\frac{C}{L}}V_1-\frac{ks}{n}\sqrt{\frac{C}{L}}V_s\right]e^{\frac{q_1 t}{T}} \qquad (42c)$$

and
$$i_2=\left[-\frac{k}{n}I_1+2s^4k^2(1-k^2)I_2+\sqrt{\frac{C}{L}}\frac{ks}{n}V_1+\sqrt{\frac{C}{L}}2s^3k^2(1-k^2)V_s\right]e^{\frac{\delta t}{T}}\cos\frac{\gamma t}{T}$$
$$+\left[+\frac{ks}{n\sqrt{1-k^2}}I_1+\frac{sk^2}{\sqrt{1-k^2}}I_2+\sqrt{\frac{C}{L}}\frac{k}{n\sqrt{1-k^2}}V_1-\sqrt{\frac{C}{L}}\frac{k^2}{n^2\sqrt{1-k^2}}V_s\right]e^{\frac{\delta t}{T}}\sin\frac{\gamma t}{T}$$
$$+\left[+\frac{k}{n}I_1+I_2-\sqrt{\frac{C}{L}}\frac{ks}{n}V_1+\sqrt{\frac{C}{L}}\frac{V_s}{sn^2}\right]e^{\frac{q_1 t}{T}}-\sqrt{\frac{C}{L}}\frac{V_s}{sn^2} \qquad (43c)$$

It will be noted that, in general, the quantities I_1, nI_2, $\sqrt{\frac{C}{L}}\,V_1$ and $\frac{1}{n}\sqrt{\frac{C}{L}}\,V_s$ will be of the same order of magnitude, although in special cases any of them may vanish. Consequently, for small values of s, equations (42c) and (43c) reduce to

$$i_1=I_1e^{\frac{\delta t}{T}}\cos\frac{\gamma t}{T}+\left[\sqrt{\frac{C}{L(1-k^2)}}\left(-V_1+\frac{k}{n}V_s\right)\right]e^{\frac{\delta t}{T}}\sin\frac{\gamma t}{T} \tag{44c}$$

$$i_2=-\frac{k}{n}I_1e^{\frac{\delta t}{T}}\cos\frac{\gamma t}{T}+\left[\frac{k}{n}\sqrt{\frac{C}{L(1-k^2)}}\left(V_1-\frac{k}{n}V_s\right)\right]e^{\frac{\delta t}{T}}\sin\frac{\gamma t}{T}$$
$$+\left(\frac{k}{n}I_1+I_2\right)e^{\frac{q_1t}{T}}-\frac{V_s}{R_2}\left(1-e^{\frac{q_1t}{T}}\right) \tag{45c}$$

These equations indicate that both the primary and secondary currents have oscillating components of frequency $\frac{\gamma}{2\pi T}$ which may have a considerable amplitude. The two currents are, however, opposite in phase so that the secondary flux turns which are given by

$$N_2\phi_2=L_2\left(i_2+\frac{ki_1}{n}\right)=L_2\left(\frac{k}{n}I_1+I_2\right)e^{\frac{q_1t}{T}}-\frac{L_2V_s}{R_2}\left(1-e^{\frac{q_1t}{T}}\right) \tag{46c}$$

do not contain any oscillatory component. Also the quantity $(i_1+n\ i_2)$ which is plotted as abscissa in the flux turn-current diagram will fluctuate only with an amplitude which is less than that of the fluctuation in the individual currents in the ratio of $1-k:1$. The state point, therefore, except for this slight oscillation, will move along its normal locus in spite of the oscillations in the currents.

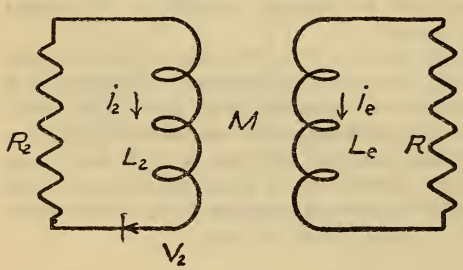

Fig. 21.—*Magnetically coupled circuits each containing inductance and resistance*

The presence of such oscillations is not shown in the usual oscillograms of the secondary current in ignition sparks. The frequency to be expected, however, is so great that an oscillograph vibrator of the usual type would not respond to them. When such a spark is viewed in a mirror rotating at high speed a quite definite series of light and dark bands is visible,[7] the spacing of which is affected by changes in the primary condenser. Presumably these bands are experimental evidence of the existence of the oscillations indicated by the foregoing theory. It will be seen from Figure 16 that δ increases rapidly with s when k^2 is nearly unity and s is small. It is therefore probable that in most cases the oscillations are damped out fairly rapidly. Although equations (46c) and (44c) suffice to locate the curve of $N_2\phi_2$ *v.* i_1 (as sketched at *RY* fig. 4), the energy involved in the oscillations is small and for most purposes it is not worth while to plot them on the diagram.

The exponential decay of i_2 and $N_2\phi_2$, indicated by the last two terms in equations (45c) and (46c), is the result of the energy used in overcoming the

[7] Morgan, T. D., Principles of Electric Spark Ignition in Internal Combustion Engines, p. 20, Crosby, Lockwood & Son, London, 1922.

resistance drops in R_2 and the voltage V_s of the arc. The effect is continued during both period 3 and period 4 and ends only at the end of period 4 when the arc ceases and conditions change abruptly to a new state to which the assumption of a constant arc voltage V_s does not apply.

The second part of the phenomenon occurring during period 3 is the transfer of energy between eddy circuits and the actual windings. To study this mathematically, we may consider the circuits shown in Figure 21. Here subscript "$_e$" indicates the eddy current circuit and subscript "$_2$" the secondary circuit. The primary circuit and effects arising from it are not considered. The basic equations for such a system are

$$L_2\frac{di_2}{dt}+M\frac{di_e}{dt}+i_2R_2+V_2=0 \tag{47c}$$

$$L_e\frac{di_e}{dt}+M\frac{di_2}{dt}+i_eR_e=0 \tag{48c}$$

Combining these and setting

$$T_2=\frac{L_2}{R_2},\ u=\frac{L_eR_2}{R_eL_2},\ M=k_e\sqrt{L_2L_e} \tag{49c}$$

gives as the differential equation for i_2

$$uT^2{}_2(1-k_e^2)\frac{di_2}{dt}+T_2(1+u)\frac{di_2}{dt}+i_2+\frac{V_2}{R_2}=0 \tag{50c}$$

The solution of this is

$$i_2=A_2e^{\lambda_1 t}+B_2e^{\lambda_2 t}-\frac{V_2}{R_2} \tag{51c}$$

where λ_1 and λ_2 are given by

$$\lambda_1,\lambda_2=-\frac{1+u}{2T_2u(1-k_e^2)}\left[1\pm\sqrt{1-\frac{4u(1-k_e^2)}{(1+u)^2}}\right] \tag{52c}$$

In applying these equations to the present case R_2 is best considered as including only the resistance of the secondary winding. It happens that in practice the potential difference between the spark-gap terminals has a nearly constant value during period 4, and hence can well be represented by assigning to the term V_2 of equation (47c) a value V_s. This voltage required to sustain the arc at the spark gap thus takes account of the energy loss in the gap and the equations need apply only while i_2 is positive.

On this basis T_e is much smaller than T_2, so that u is quite small. Values determined on a group of 10 ignition systems ranged from

$$u=0.0025 \text{ to } u=0.017$$

Hence the radical in equation (52c) can be expanded to give

$$\lambda_1=-\frac{1}{T_2u(1-k_e^2)}=-\frac{1}{T_e(1-k_e^2)} \tag{53c}$$

$$\lambda_2=-\frac{1}{T_2} \tag{54c}$$

Also, if we assume for convenience $L_e=L_2$, since we care only about the magnetic effects of i_e and not about its absolute magnitude we get

$$i_e=A_e e^{\lambda_1 t}+B_e e^{\lambda_2 t} \tag{55c}$$

Inserting the values of the constants A_2, B_2, A_e and B_e we get if u is small compared to 1

$$i_2=\left(k_e^2\frac{V_s}{R_e}-k_eI_e\right)e^{\lambda_1 t}+\left(I_2+k_eI_e-k_e^2\frac{V_s}{R_e}+\frac{V_s}{R_2}\right)e^{\lambda_2 t}-\frac{V_s}{R_2} \tag{56c}$$

$$i_e=\left(I_e-\frac{k_eV_s}{R_e}\right)e^{\lambda_1 t}+k_e\frac{V_s}{R_e}e^{\lambda_2 t} \tag{57c}$$

Where I_2 and I_e are the initial values of i_2 and i_e, respectively.

Since λ_1 is much larger than λ_2 (by a factor $\frac{1}{(1-k_e^2)u}$ which equals 200 if $k_e^2=0.5$ and $u=0.01$), the terms involving $e^{\lambda_1 t}$ will become negligible in a very short time and before the factor $e^{\lambda_2 t}$ has become appreciably less than unity. For the 10 systems studied λ_1 ranged from 2×10^{-4} to 8.5×10^{-4}. The currents, therefore, arrive at the values indicated by the $e^{\lambda_2 t}$ and the constant terms, in about 1/10,000 second after the spark has started. From this time on the current through the spark gap will drop off linearly with time at a rate given by

$$\frac{di_2}{dt}=-\frac{V_s}{L}\text{ approximate.} \tag{58c}$$

while the eddy current remains substantially constant. As is pointed out in Appendix D the "constant" R_e of the eddy circuit in effect depends upon the distribution of the currents and tends to decrease as the currents "soak" into the lamination. Such a decrease in R_e as shown by equation (57c) will tend to make the eddy currents increase in value during period 4 while the current in the coil drops off somewhat more rapidly than the linear relation of equation (58c) would indicate. These tendencies are quite noticeable in the sample diagrams.

APPENDIX D. EDDY CURRENTS IN INDUCTION COILS

Even a qualitative study of the electrical behavior of ignition apparatus reveals numerous features which can be most readily explained by assuming the presence of eddy currents in the iron core and other metallic masses located in its magnetic field. It is the purpose of this note to discuss qualitatively the probable nature of these currents from a point of view which is somewhat different from, though not inconsistent with, the treatment given elsewhere in this paper.

While the actual effect of eddy currents is made up of contributions from the currents in various parts of the machine which differ greatly in dimensions, permeability, etc., a general idea can be obtained by considering the phenomena in one piece which for definiteness may be thought of as a lamination adjacent to the windings.

In Figure 22 is a series of sketches indicating schematically the occurrences during the magneto cycle in such a lamination. *A–E* indicates the iron core, *E–C* the primary winding, and *C–D* the secondary winding, *AX* being the center line of the lamination.

During period 1 conditions are as in Figure 22(*a*). The flux density *B* is substantially uniform throughout the thickness of the iron, and changes only very slowly with time. The primary current, shown at i_1, builds up gradually to about the extent needed to maintain *B* in spite of the motion of the core with respect to the magnets. At the end of period 1 it exerts a definite mag-

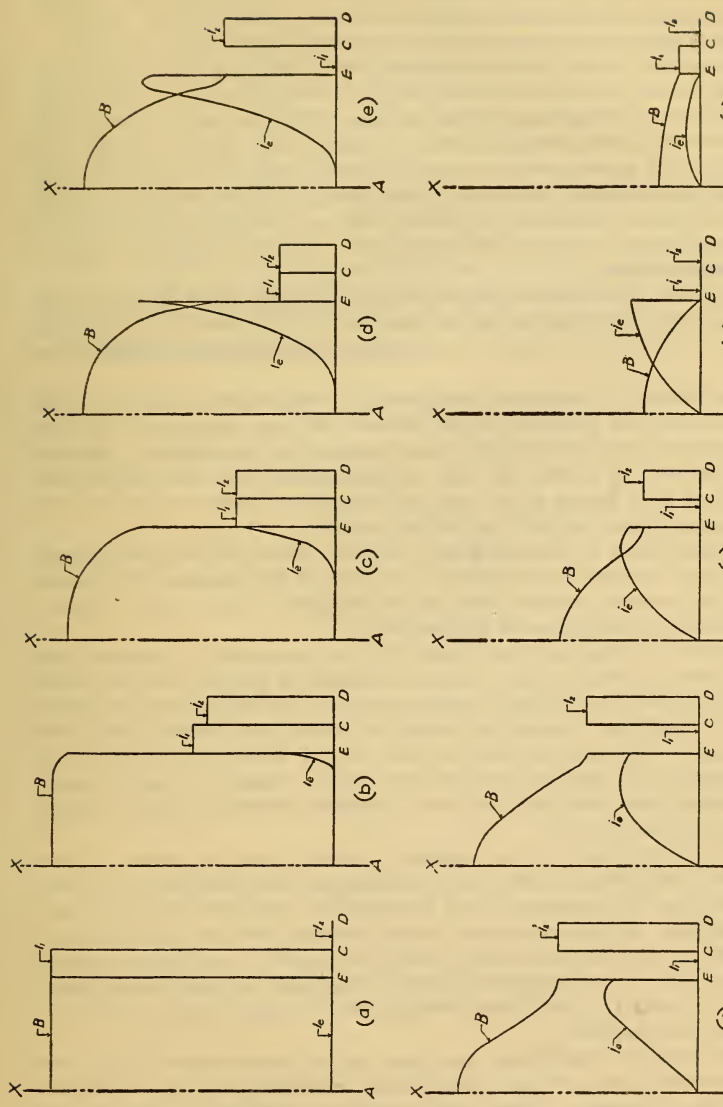

Fig. 22.—*Sketches showing qualitatively by curves "B" the distribution of magnetic flux, and by curves "i_e" the density of eddy-currents, within the thickness of a single iron lamination. Each sketch corresponds to a time when the primary and secondary currents have the relative values shown by "i_1" and "i_2" respectively.* (a) *is for period 1;* (b), (c), (d) *for period 2;* (e) *for period 3;* (f), (g), (h) *for period 4;* (i) *for period 5; and* (j) *for period 6*

netomotive force. (In a typical case this may be 800 ampere turns.) The induced emf per turn is small (probably not over 0.01 volt) and the eddy current i_e is practically zero.

During period 2 the breaker contacts are open. i_1 decreases very rapidly while i_2 builds up at first to the condition shown in Figure 22 (*b*). Both currents then decrease as they charge their respective capacitances as shown in Figures 22 (*c*) and (*d*). These abrupt changes in magnetomotive force cause a tendency toward a decrease in flux density to start inward into the core material. The rate of decrease of flux increases with time and the emf which it produces both in the windings and in the metal may become as great as 2 volts per turn of winding. This emf causes a corresponding wave of eddy currents in the outer part of the core. The direction of flow of these currents is such as to tend to maintain the original flux and to check the progress of the demagnetization, and their magnetomotive force may amount to several hundred ampere turns.

Because of the short time which has elapsed the eddy currents have appreciable values only near the surface of each piece of iron and may be thought of as being induced in a circuit of relatively high resistance and low time constant.

Their distribution is therefore quite similar to that which is obtained if the winding is energized with alternating current of high frequency. At 3,000 cycle the effective penetration[8] into sheet material of permeability 1,000 and resistivity 10,000 cgs is only 0.1 mm. Experimental data with currents of this frequency have shown in the case of 10 ignition systems values of time constant ranging from 0.2×10^{-4} to 1.2×10^{-4} seconds.

The breaking down of the spark gap serves to close the secondary circuit through a path of fairly low resistance. Because of the presence of its series condenser the primary current soon ceases altogether and we have momentarily conditions somewhat as in Figure 22 (*e*).

As is shown by equations (56c) and (57c) of Appendix C, whenever two circuits of widely different time constants embrace a common core in which the flux is dying out the relative currents in the two circuits adjust themselves rapidly to a condition in which the circuit of greater time constant has most of the current. The rate of decay of flux is now sufficient to give in the secondary an emf of only about 0.1 volt per turn. Hence, the high intensity of eddy current must also drop, while the secondary current increases further, as shown in Figure 22 (*f*).

Actually the increases of the secondary current from the decay of both eddy current and primary current are simultaneous, and probably very rapid, so that condition (*f*) is reached early in period 4. From this point on, however, the decrease of flux has time to spread into the core and is accompanied by a growth of eddy current in the inner parts, while the secondary current drops off steadily as the magnetic energy is dissipated as heat in the spark Conditions (*g*) and (*h*) are passed through and the spark dies out while the eddy current still persists.

It is now, however, distributed over most of the cross section of the core in about the same way as the eddy current resulting from an alternating current of low frequency. Tests with currents of frequencies down to 200 cycles per second show decidedly higher values for the effective time constant of the eddy-current circuits in typical ignition systems. At 200 cycles the values for a group of 10 such systems tested were found to range from

[8] Jeans, J. H., Electricity and Magnetism, 3d ed., p. 479.

0.4×10^{-4} to 9×10^{-4} seconds, and presumably for very slow changes the values would be still greater.

Hence, the induced emf of 0.1 volt per turn may maintain a total eddy current which is quite comparable with that existing at the end of period 2 when a higher emf was acting on a circuit of much higher resistance.

After the spark has died out we have, during period 5, the condition of Figure 22 (*i*) in which eddy currents alone are flowing. Their presence is manifested on an oscillogram of primary voltage (see fig. 10 and fig. 13a) by the curve of decay between the end of the spark *J* and the closing of the breaker *A'*. Circuit time constants computed from such decay curves are in fair agreement with those deduced from a. c. measurements. The dotted lines in Figures 8 and 9 indicate the probable magnitude of such currents under the conditions then existing.

When the breaker contacts close at the beginning of period 1, the primary circuit of very low resistance and high time constant again is closed around the core. The bulk of the eddy current again transfers to the primary circuit as indicated by Figure 22 (*j*) and at *A'* in Figure 13 (*b*).

WASHINGTON, June 14, 1926.